ABRACADABRA from Axions to Gravitational Waves

Kaliroë Pappas
MIT Laboratory for Nuclear Sciences
Winslow Group

August 7, 2024

Axion Signal

Gauss-Ampère law

$$\partial_\nu F^{\mu\nu} = j^\mu_{eff}$$

Axions Modification:

$$j^\mu_{eff} = \partial_\nu\left(g_{a\gamma\gamma} a \tilde{F}^{\nu\mu}\right)$$

$$\downarrow$$

$$J_{eff} = g_{a\gamma\gamma}\sqrt{\rho_{DM}}\cos(m_a t)B$$

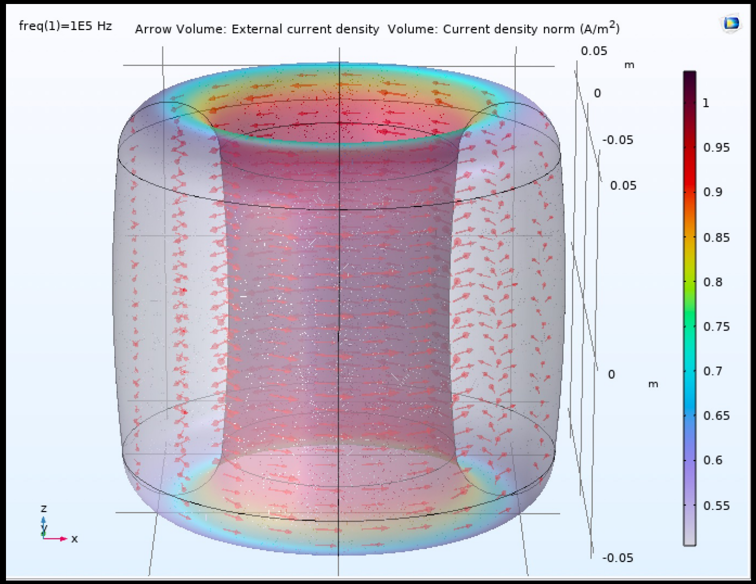

Axion effective current in the ABRA magnetic volume

Axion Signal

Gauss-Ampère law

$$\partial_\nu F^{\mu\nu} = j^\mu_{eff}$$

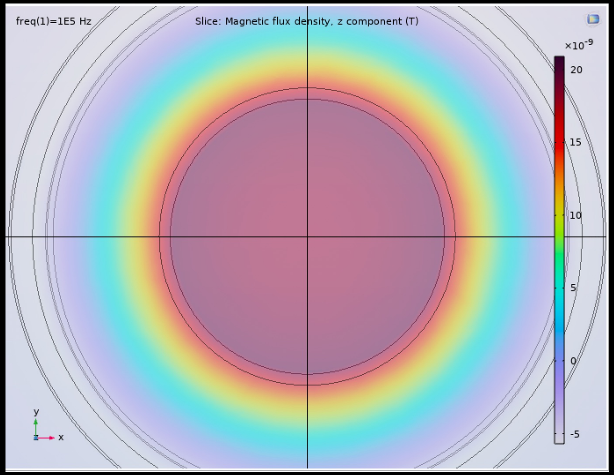

The z-component of the magnetic field resulting from an axion effective current

Axions Modification:

$$j^\mu_{eff} = \partial_\nu\left(g_{a\gamma\gamma} a \tilde{F}^{\nu\mu}\right)$$

$$\downarrow$$

$$J_{eff} = g_{a\gamma\gamma}\sqrt{\rho_{DM}}\cos(m_a t)B$$

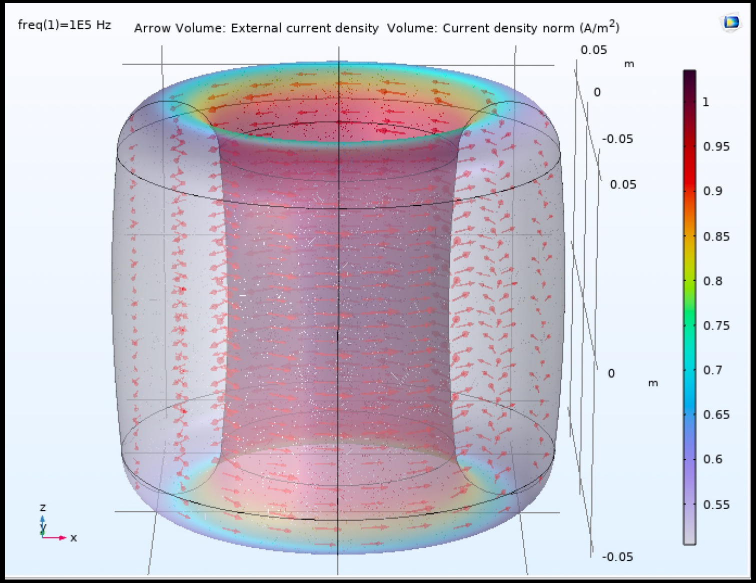

Axion effective current in the ABRA magnetic volume

Gravitational Wave Signal

Gauss-Ampère law

$$\partial_\nu F^{\mu\nu} = j^\mu_{eff}$$

Gravitational Wave Modification:

$$j^\mu_{eff} = \partial_\nu \left(-\frac{1}{2} h F^{\mu\nu} + F^{\mu\alpha} h^\nu_\alpha - F^{\mu\nu} h^\mu_\alpha \right)$$

Gravitational Wave Signal

Gauss-Ampère law

$$\partial_\nu F^{\mu\nu} = j^{\mu}_{eff}$$

Gravitational Wave Modification:

$$j^{\mu}_{eff} = \partial_\nu \left(-\frac{1}{2} h F^{\mu\nu} + F^{\mu\alpha} h^{\nu}_{\alpha} - F^{\mu\nu} h^{\mu}_{\alpha} \right)$$

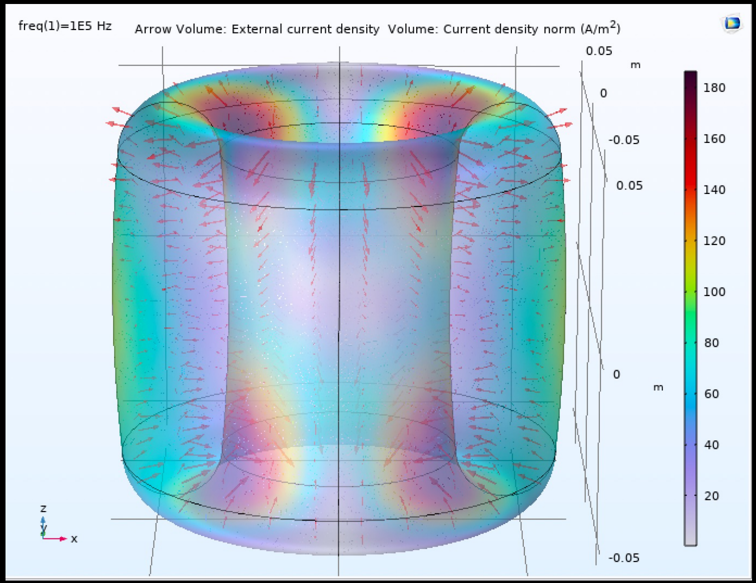

GW effective current in the ABRA magnetic volume

Gravitational Wave Signal

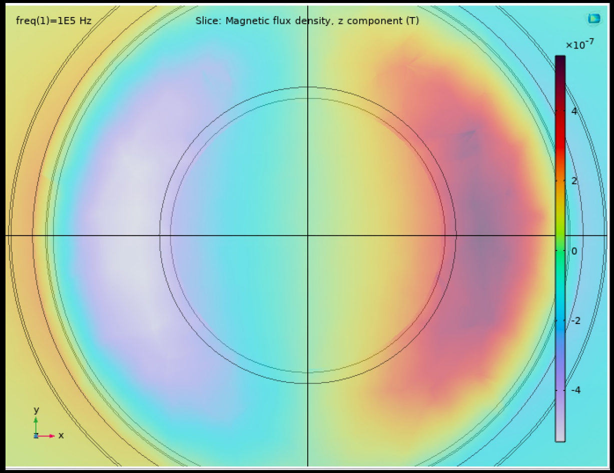

The z-component of the magnetic field resulting from a GW effective current

Gauss-Ampère law

$$\partial_\nu F^{\mu\nu} = j^\mu_{eff}$$

Gravitational Wave Modification:

$$j^\mu_{eff} = \partial_\nu\left(-\frac{1}{2}hF^{\mu\nu} + F^{\mu\alpha}h^\nu_\alpha - F^{\mu\nu}h^\mu_\alpha\right)$$

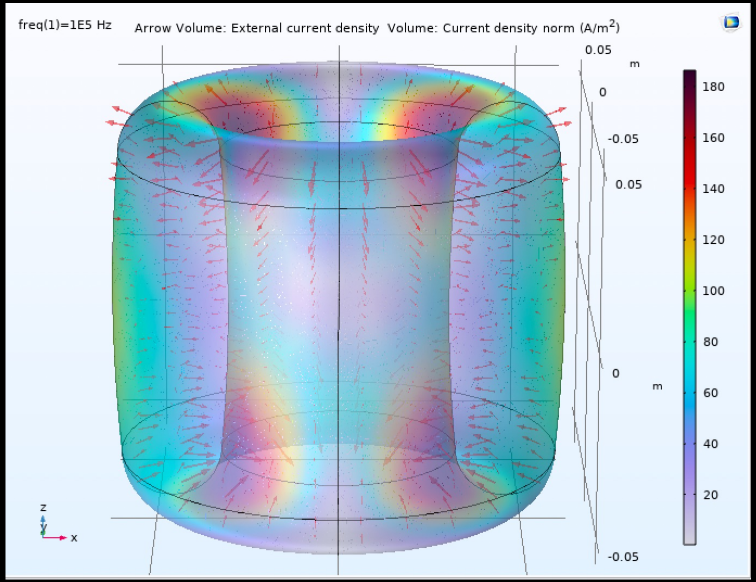

GW effective current in the ABRA magnetic volume

Experimental Setup

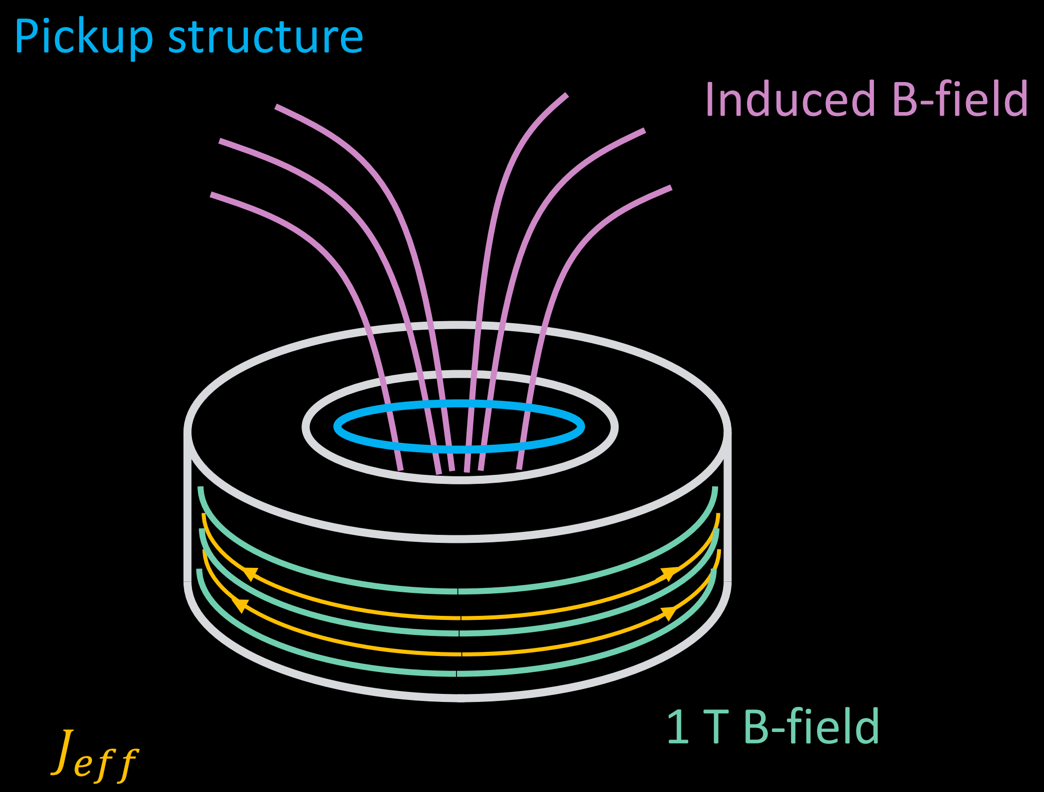

Top-down view

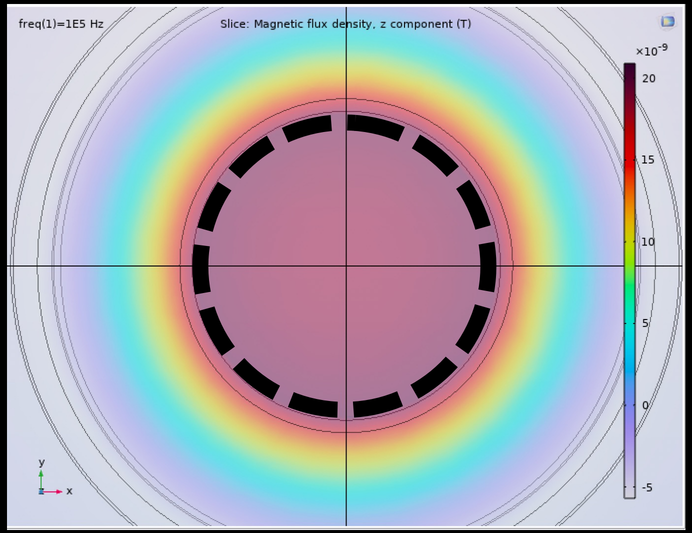

The z-component of the magnetic field resulting from an axion effective current

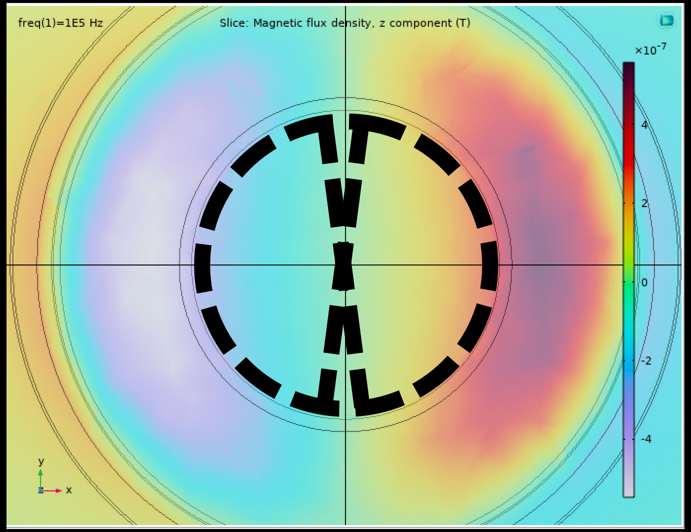

The z-component of the magnetic field resulting from a GW effective current

1. Directional search

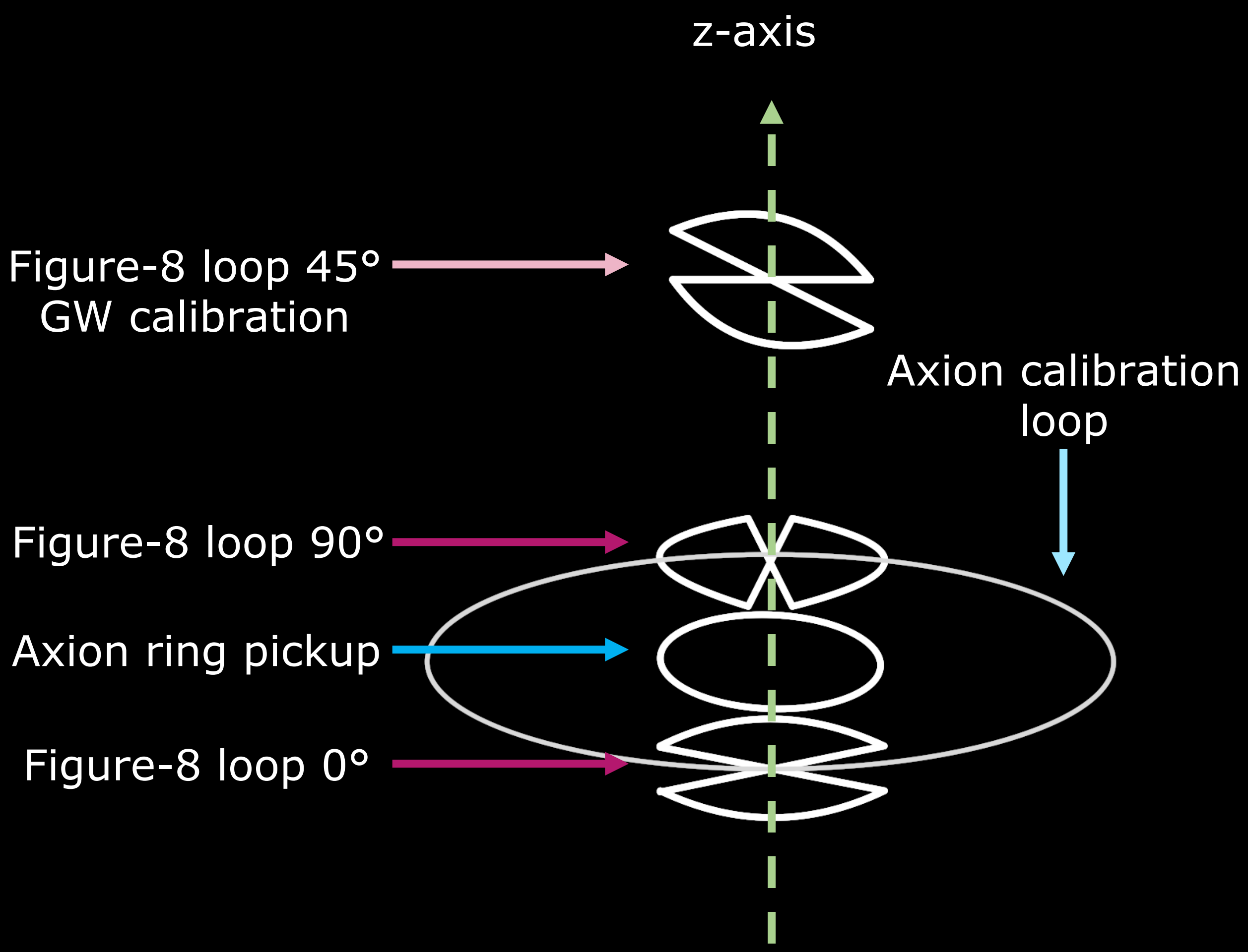

The pickup structures and calibration structures that are used in the GW axion run

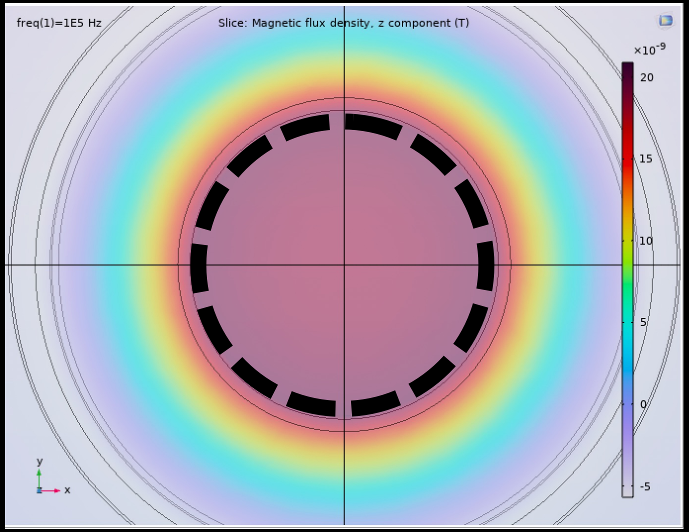

The z-component of the magnetic field resulting from an axion effective current

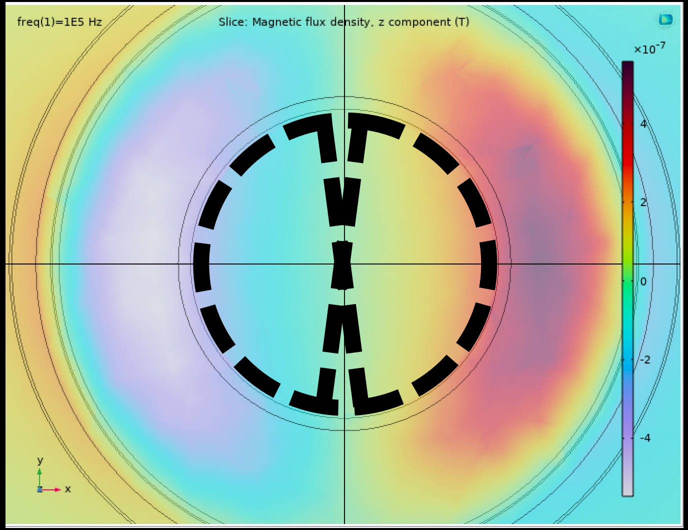

The z-component of the magnetic field resulting from a GW effective current

Calibration an axion-GW run

- To prove we can run a simultaneous axion and GW run, we must demonstrate that the GW search and the axion search can be calibrated independently
- We have four calibrations:

1. GW pickup calibrated with GW signal (GW end-to-end)
2. Axion pickup calibrated with axion signal (axion end-to-end)
3. GW pickup calibrated with axion signal (GW cross calibration)
4. Axion pickup calibrated with GW signal (axion cross calibration)

GW pickup: axion signal cross calibration

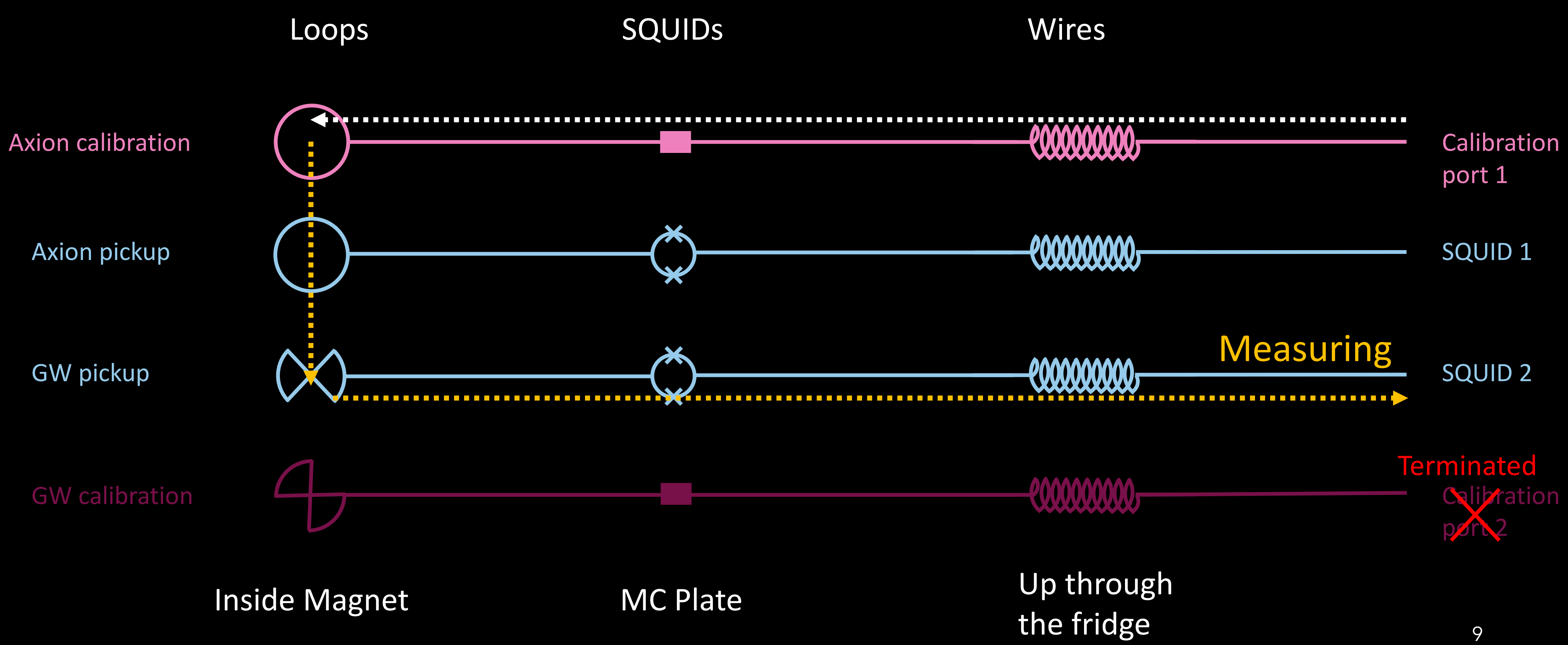

GW pickup: GW signal end-to-end calibration

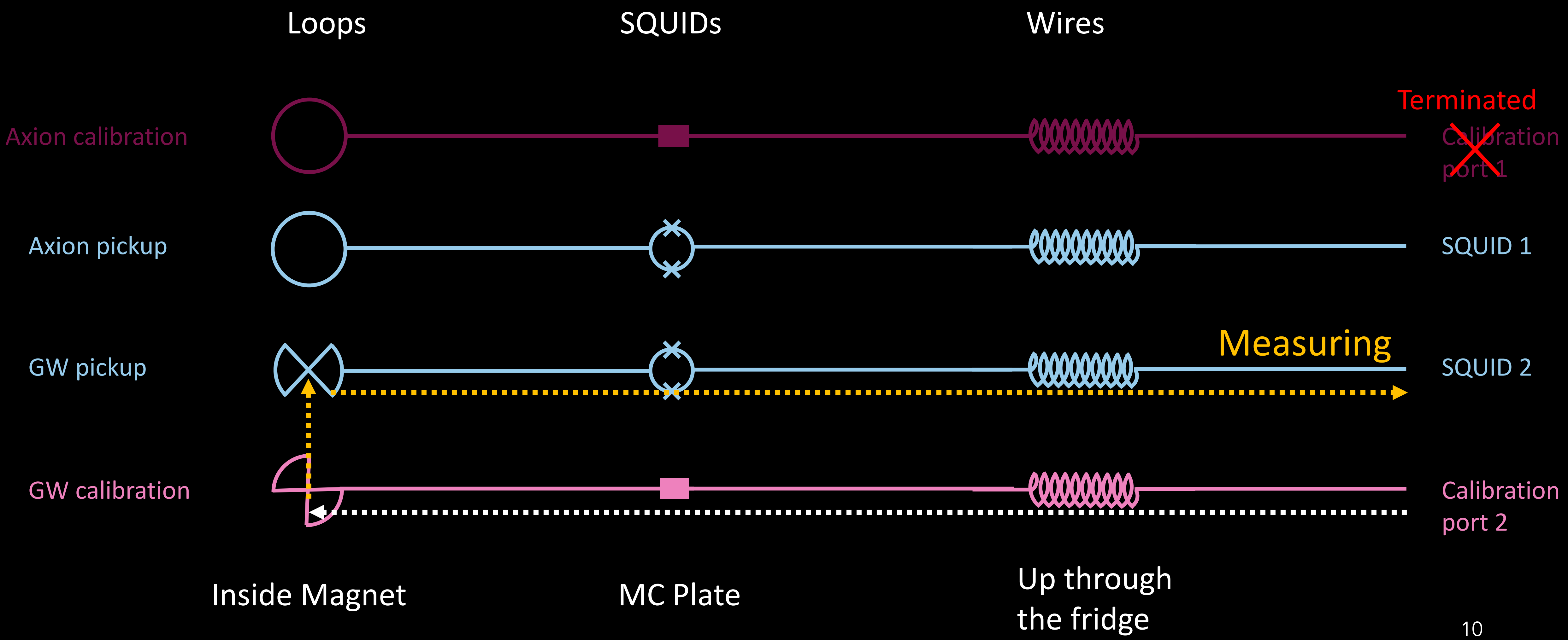

Calibration on GW pickup

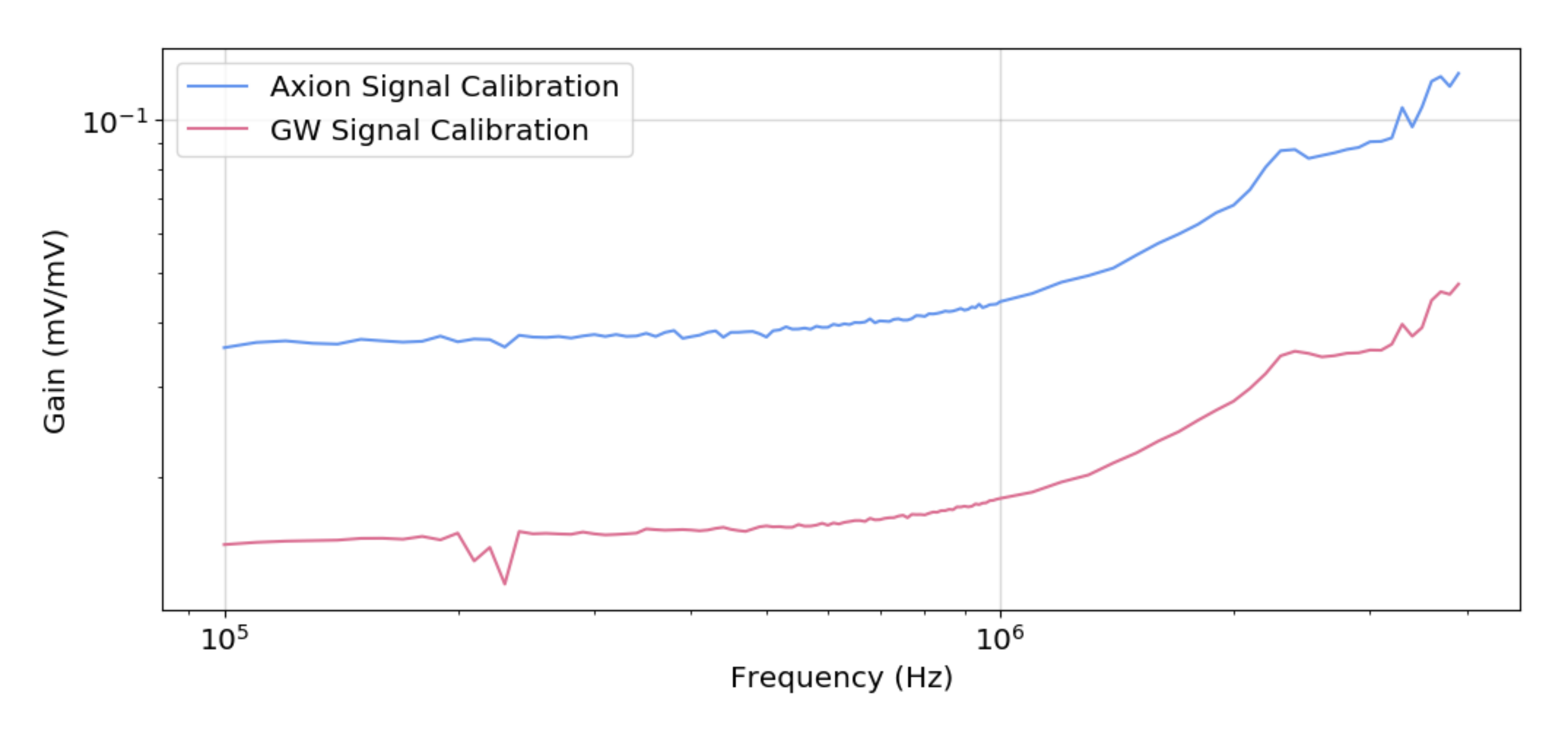

Axion to GW mutual inductance

We expect (to first order) zero mutual inductance between the figure-8 and the circle

However, we see a high amount of correlation between the signals

- Somewhere in our system there was an unknown high amount of parasitic induction
  - Pickups or twisted pairs
  - SQUIDs
  - Wires

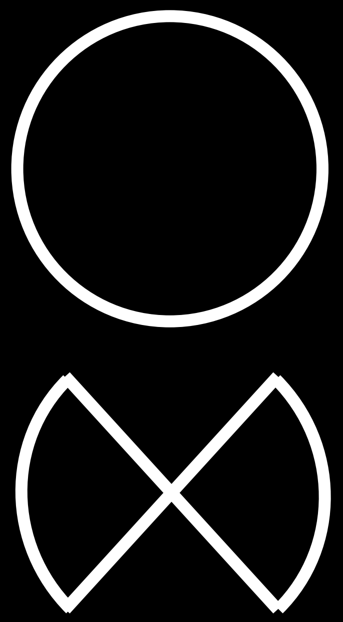

GW pickup: axion signal cross calibration

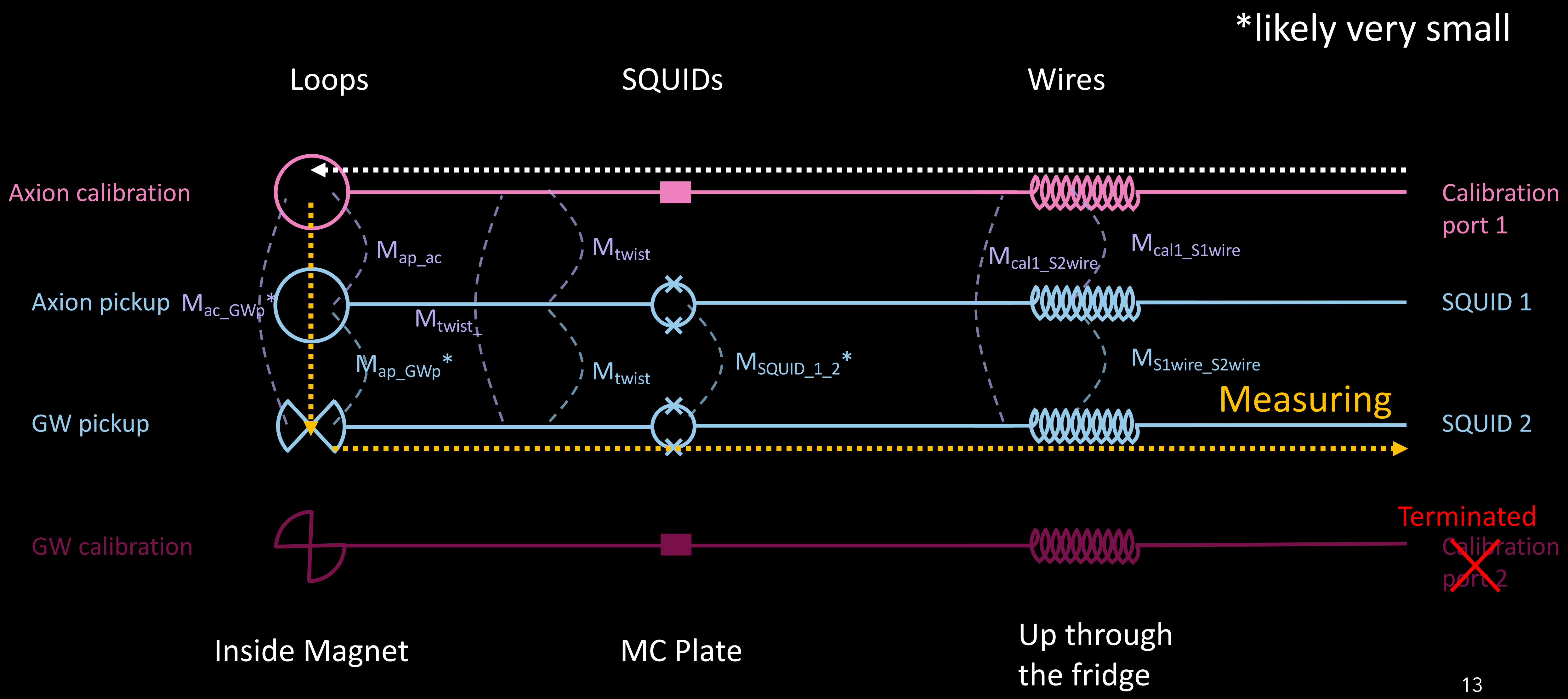

Parasitic inductance run

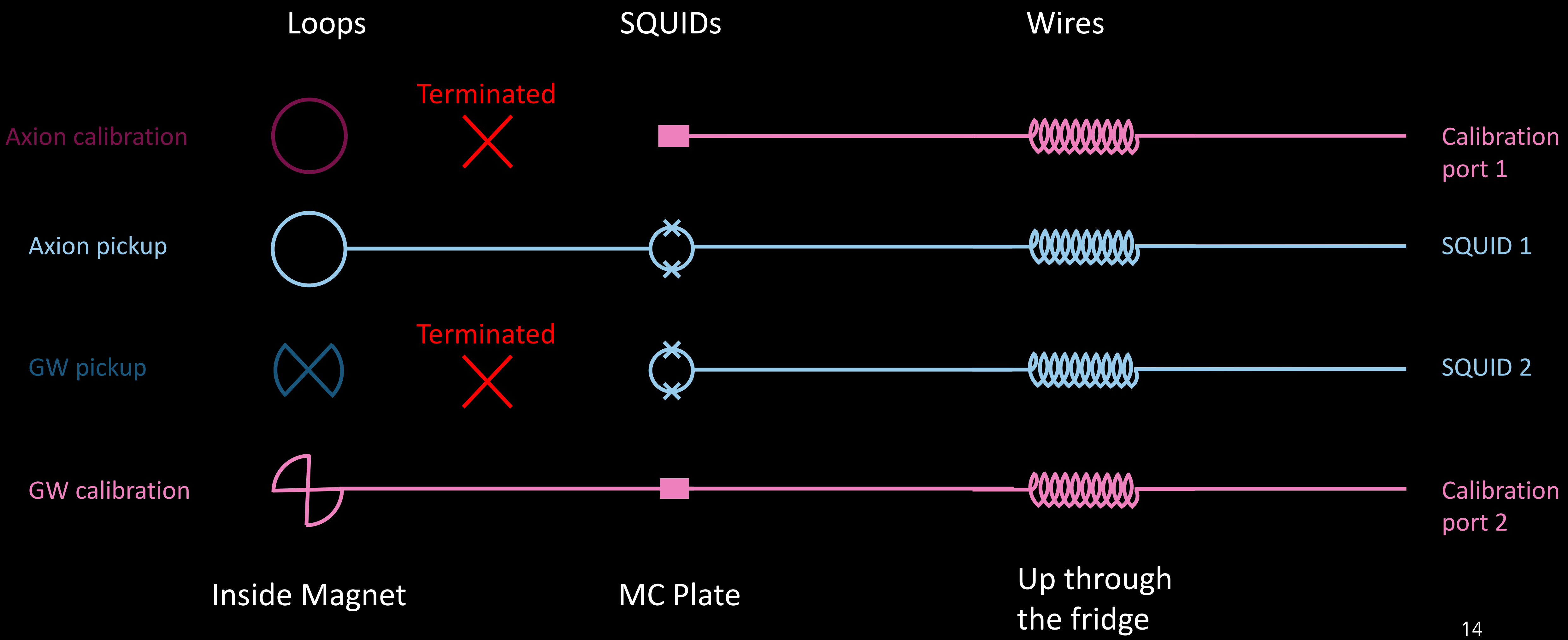

Disconnected cross calibration

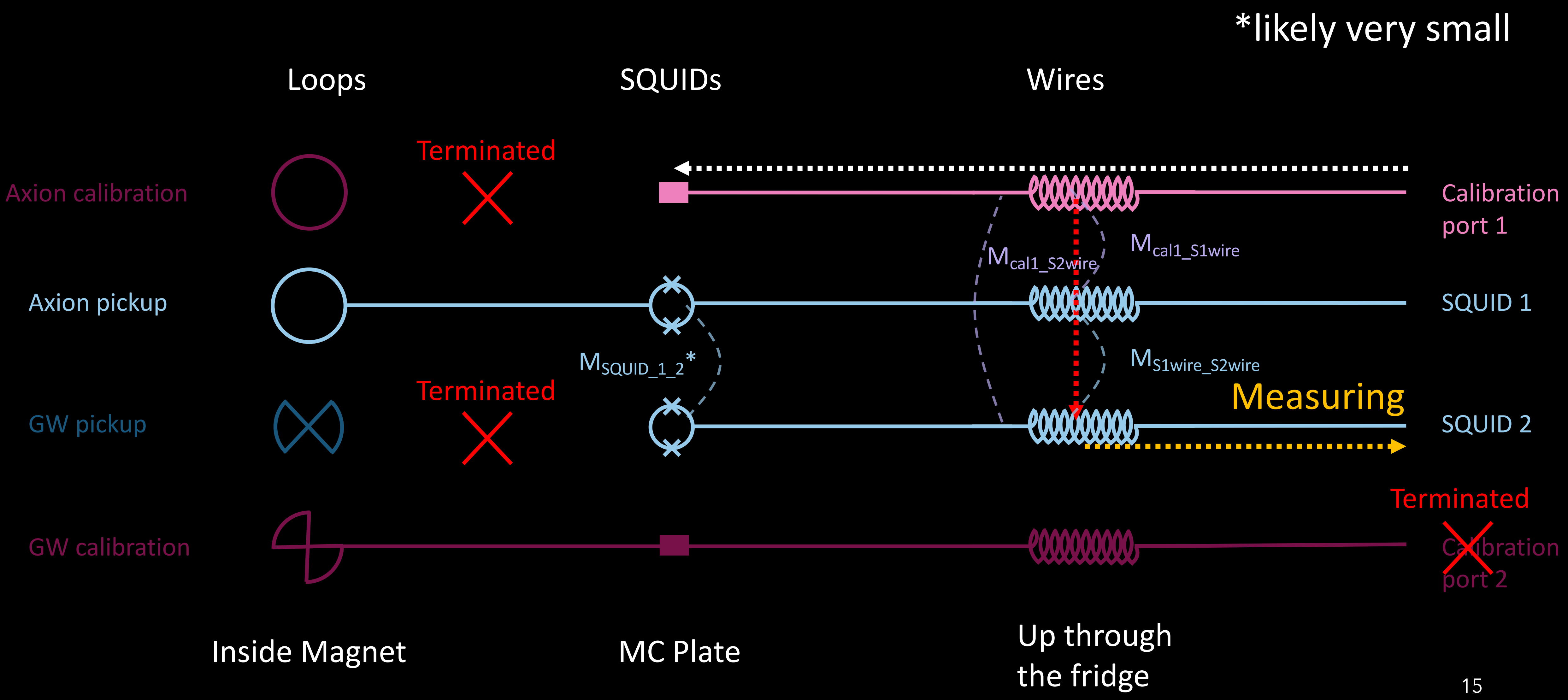

Connected cross calibration

*likely very small

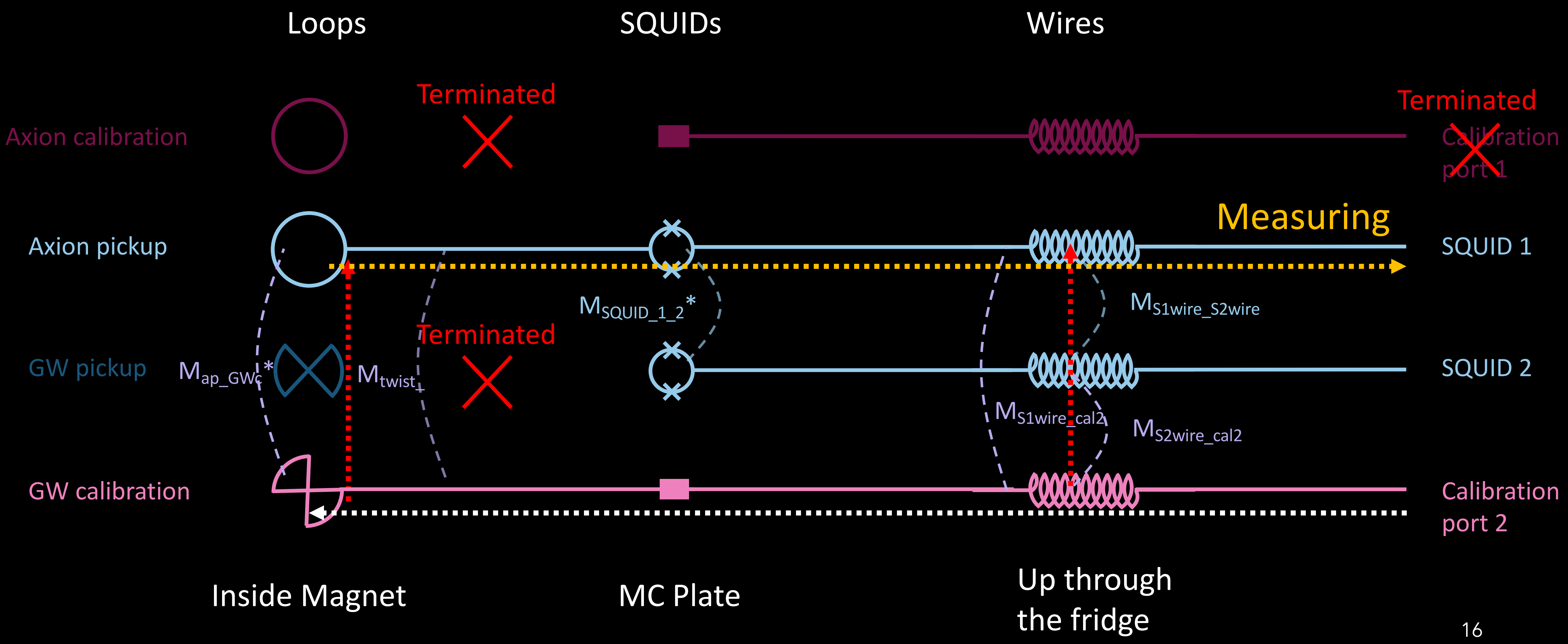

Inductance run results

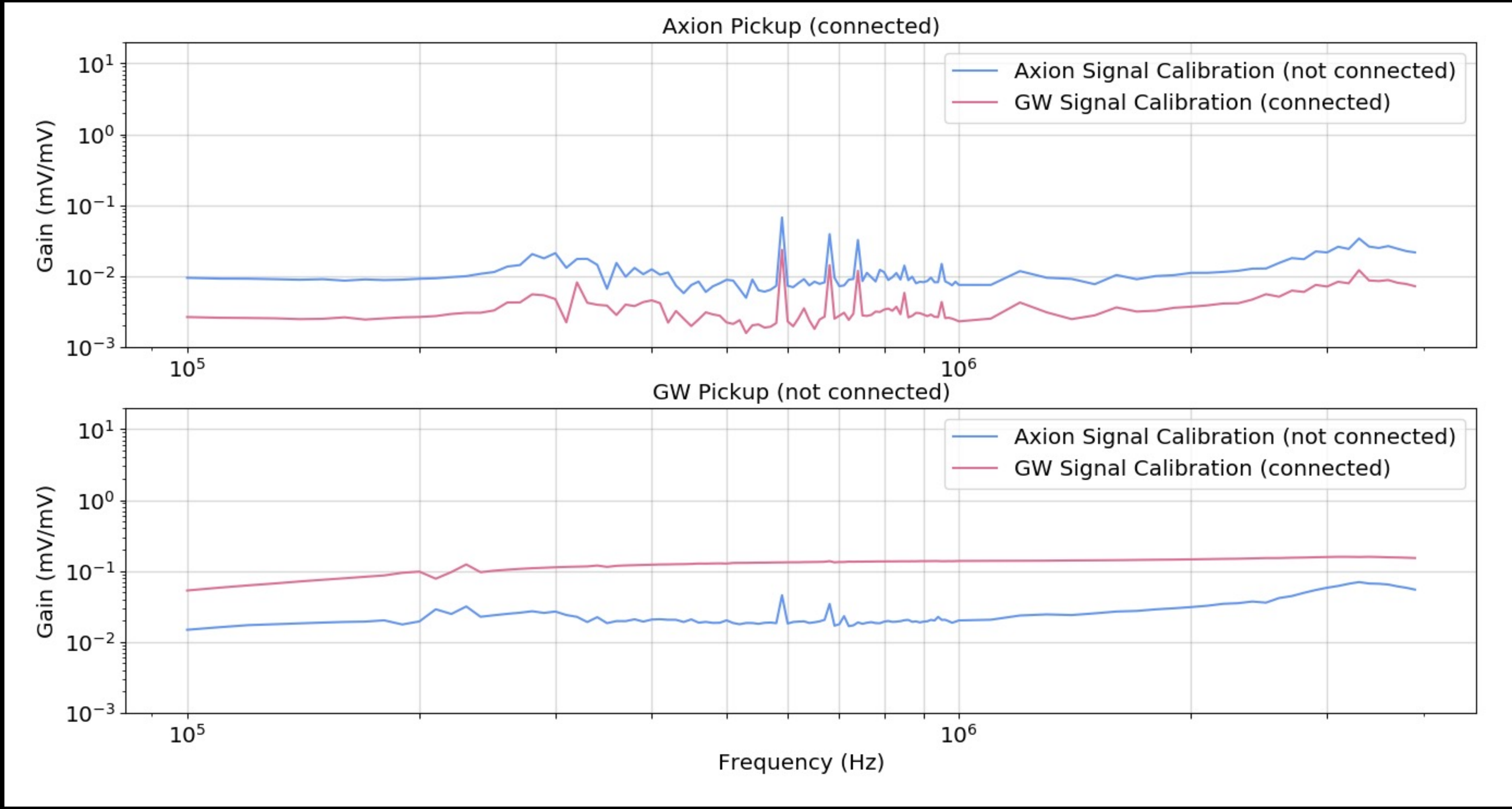

Inductance schema of all possible calibration inductances

*likely very small

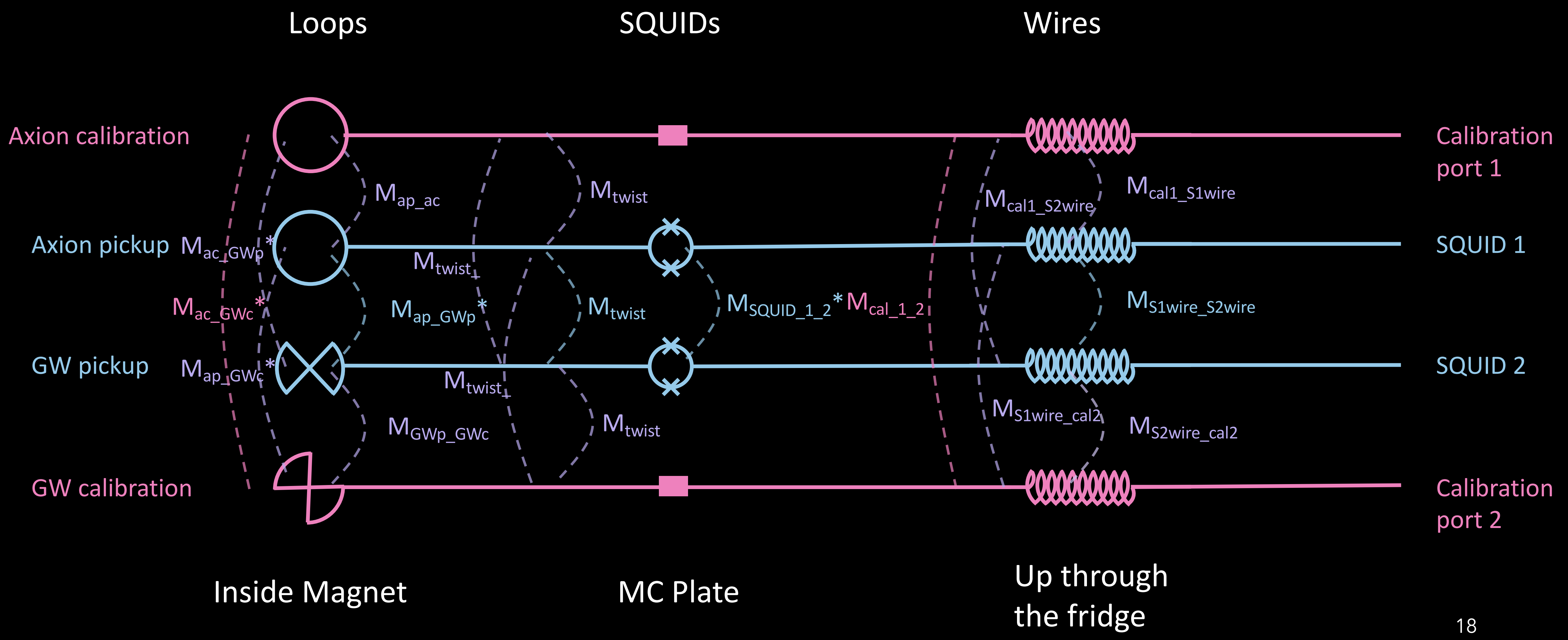

Inductance schema of all possible calibration inductances

*likely very small

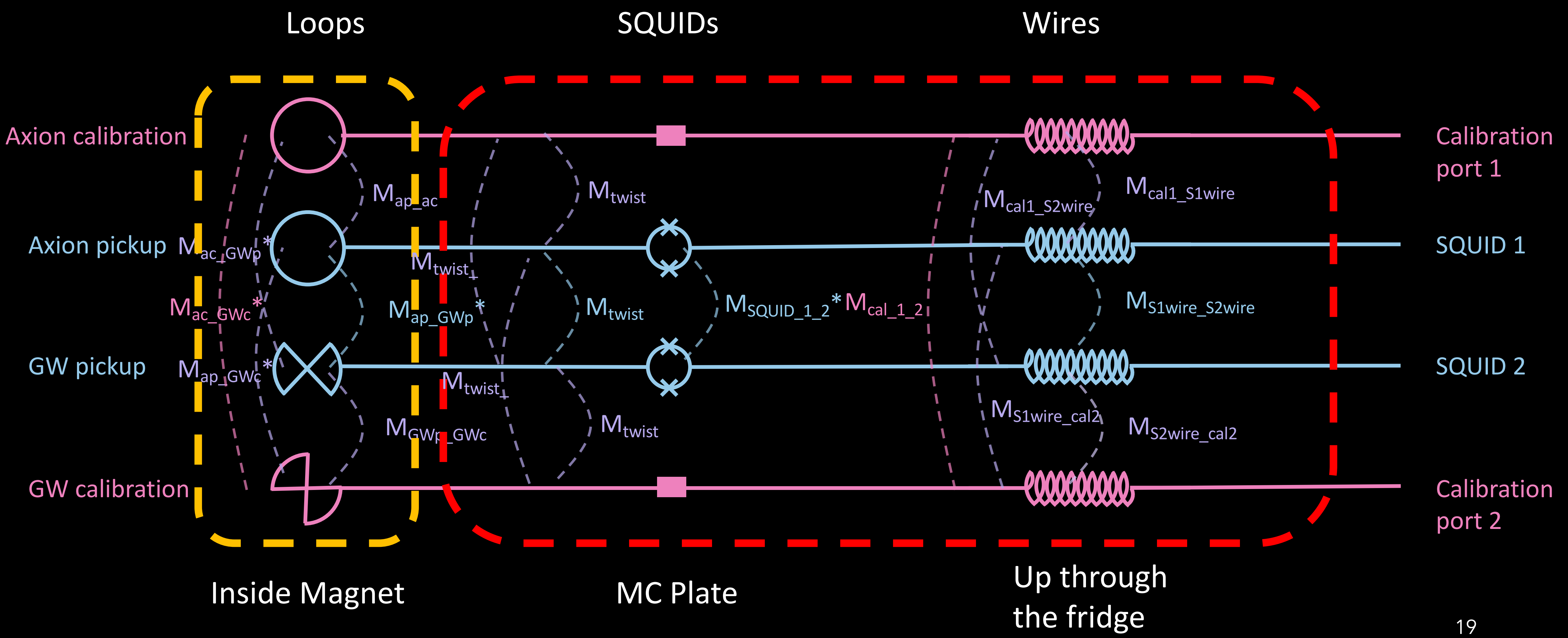

Changes made

Loops were reduced

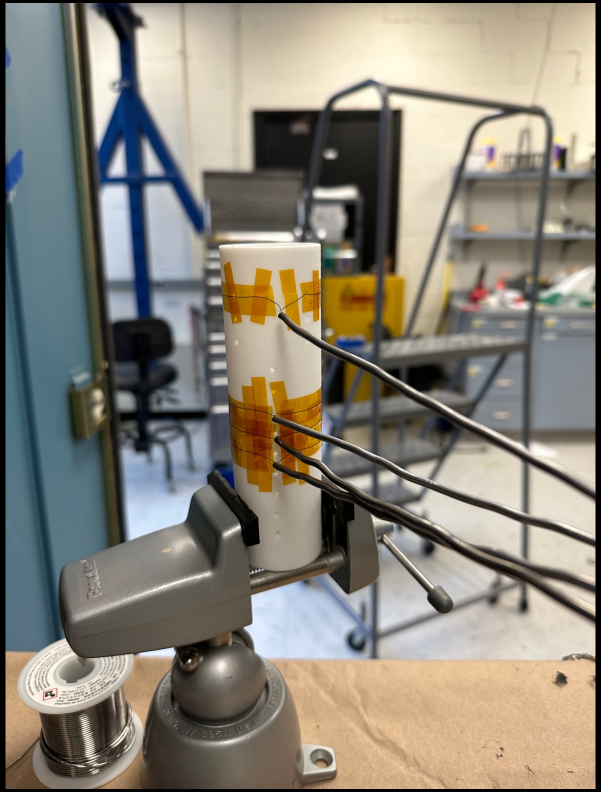

Configuration 1

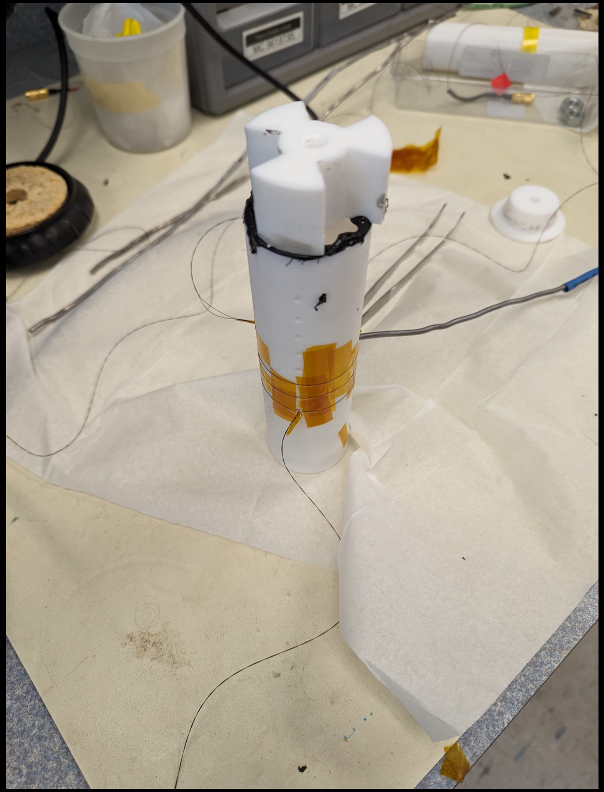

Configuration 2

Changes made

GW calibration loop moved closer to GW pickup

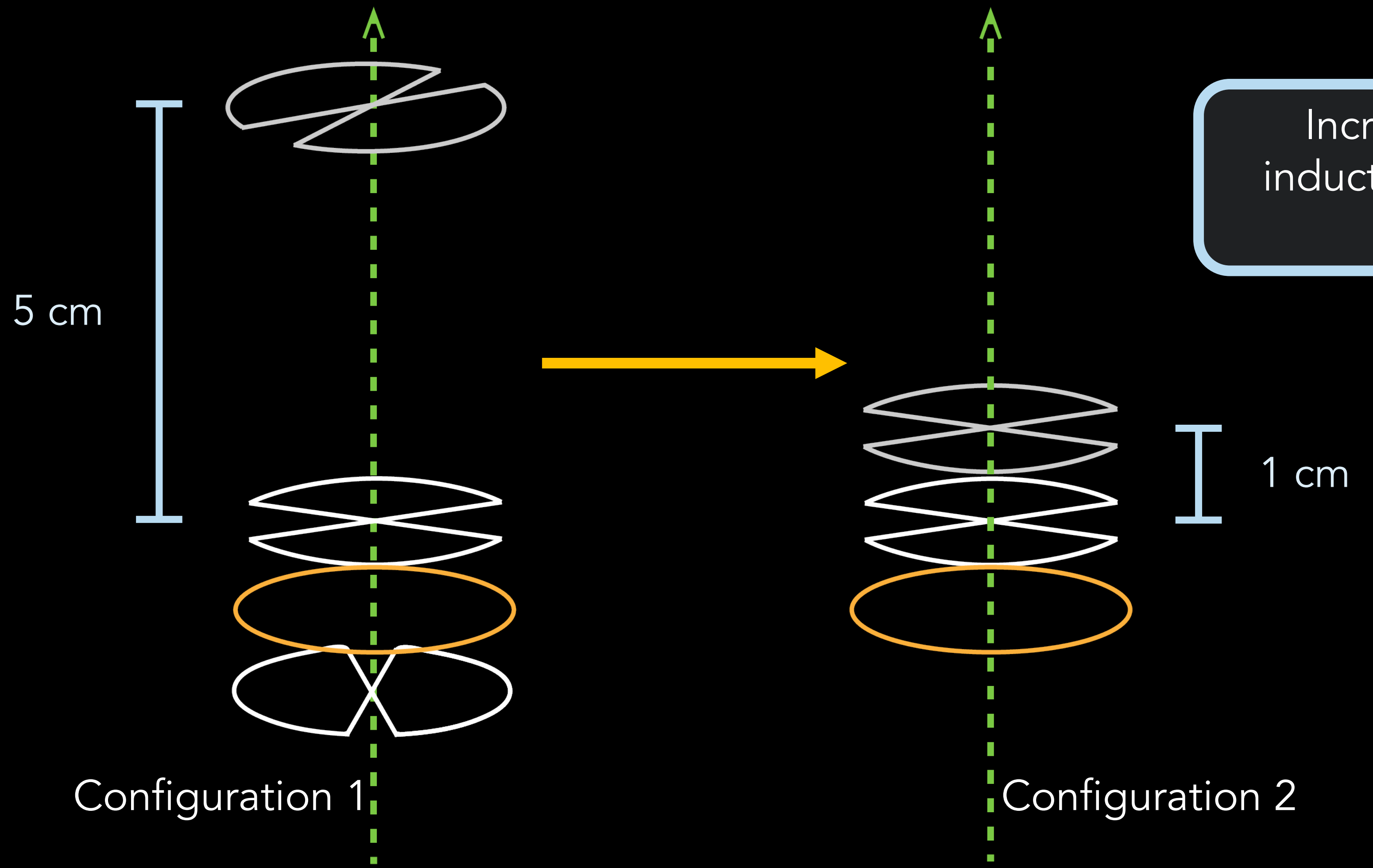

Increased our mutual inductance by 2 orders of magnitude

Changes made

Twisted pairs distanced

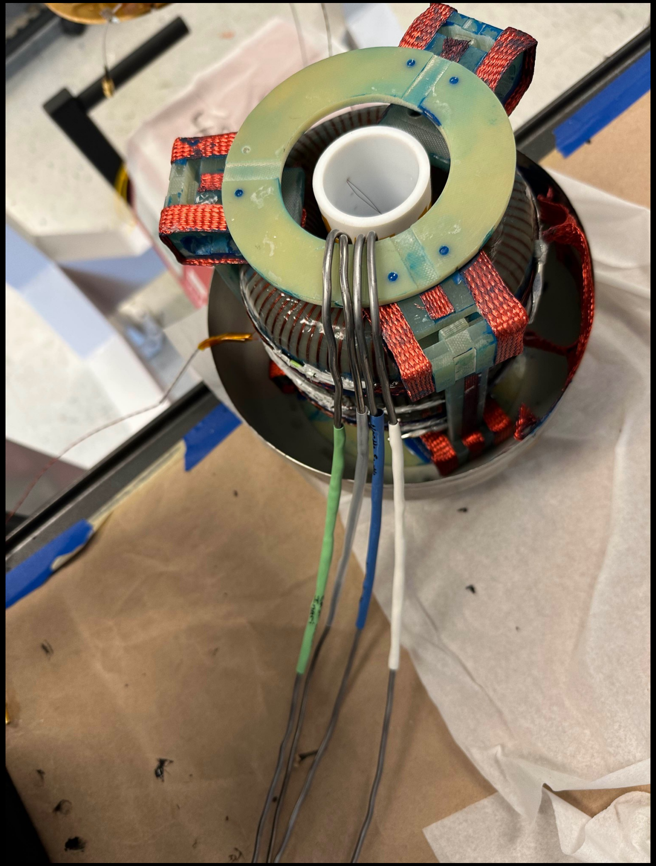

Configuration 1

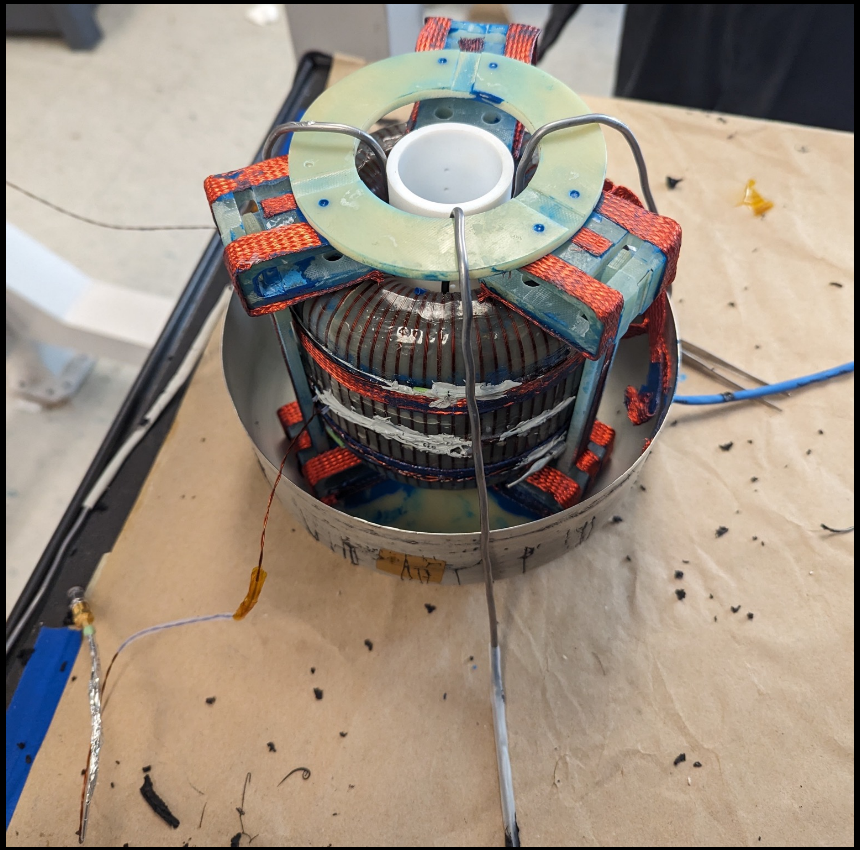

Configuration 2

Experimental Setup

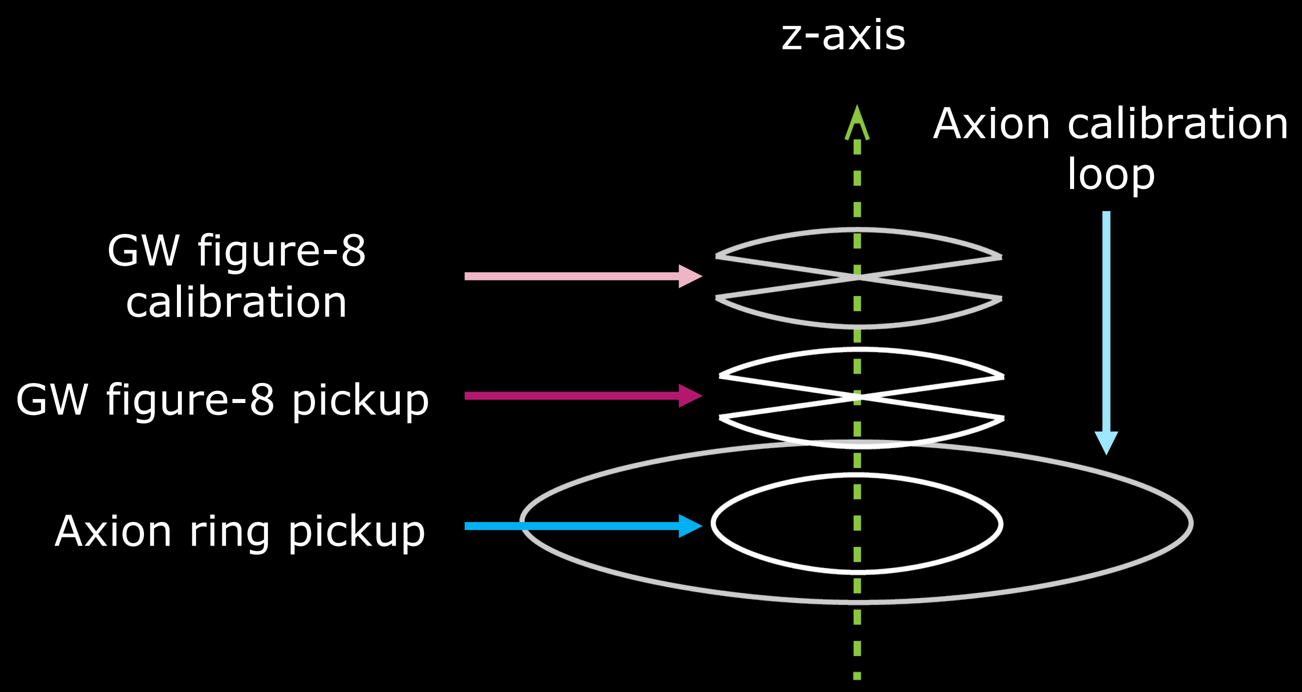

The pickup structures and calibration structures that are used in the GW axion run

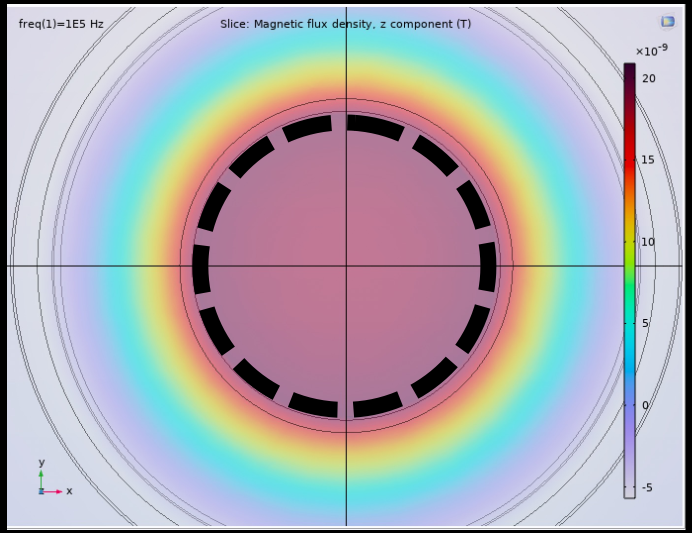

The z-component of the magnetic field resulting from an axion effective current

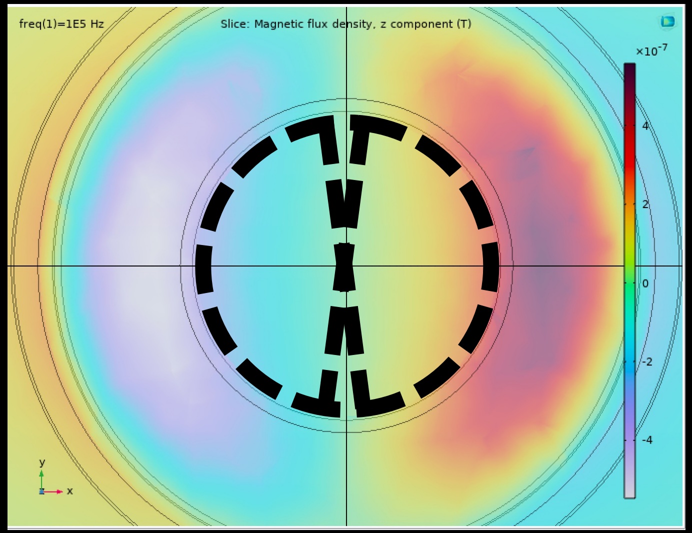

The z-component of the magnetic field resulting from a GW effective current

GW pickup calibration results from configurations 1 & 2

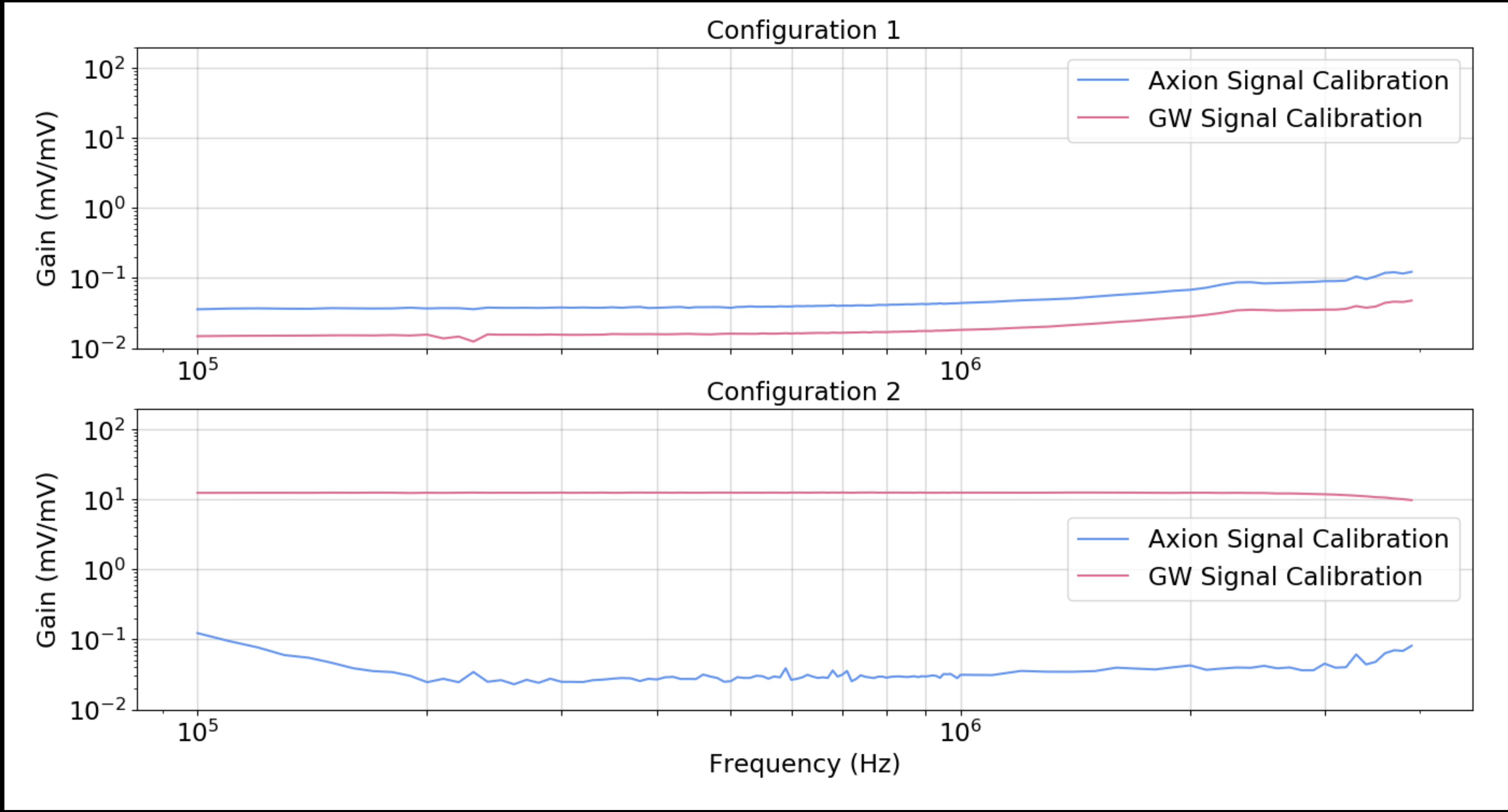

Signals and Data

ABRA-GW Goals

1. Maintain sensitivity to axions
2. Achieve the projected GW sensitivity
3. Perform pathfinder analysis

Gravitation Waves

Proposed by Einstein, moving masses create propagating oscillations in the gravitational field

First detected by LIGO/VIRGO in 2016 (2017 Nobel Prize)

$F < 10$ kHz $\longrightarrow$ Mergers of black holes and neutron stars

New physics > 10 kHz such as:

- **Primordial blackhole binaries**
- Superradiance
- Cosmology

Primordial Black Hole Merger Templates

Using the ripple code base to create the wave-forms of the merger

Merger parameter	value
M_1	$0.01\ M_\odot$
M_2	$0.01\ M_\odot$
Dimensionless spin	0
Time of coalescence	1 ms
Distance to source	$3.24 \times$ 1e-23 Mpc (1 m)
Inclination	0

Template Transformation

Need to transform the template into the detector frame

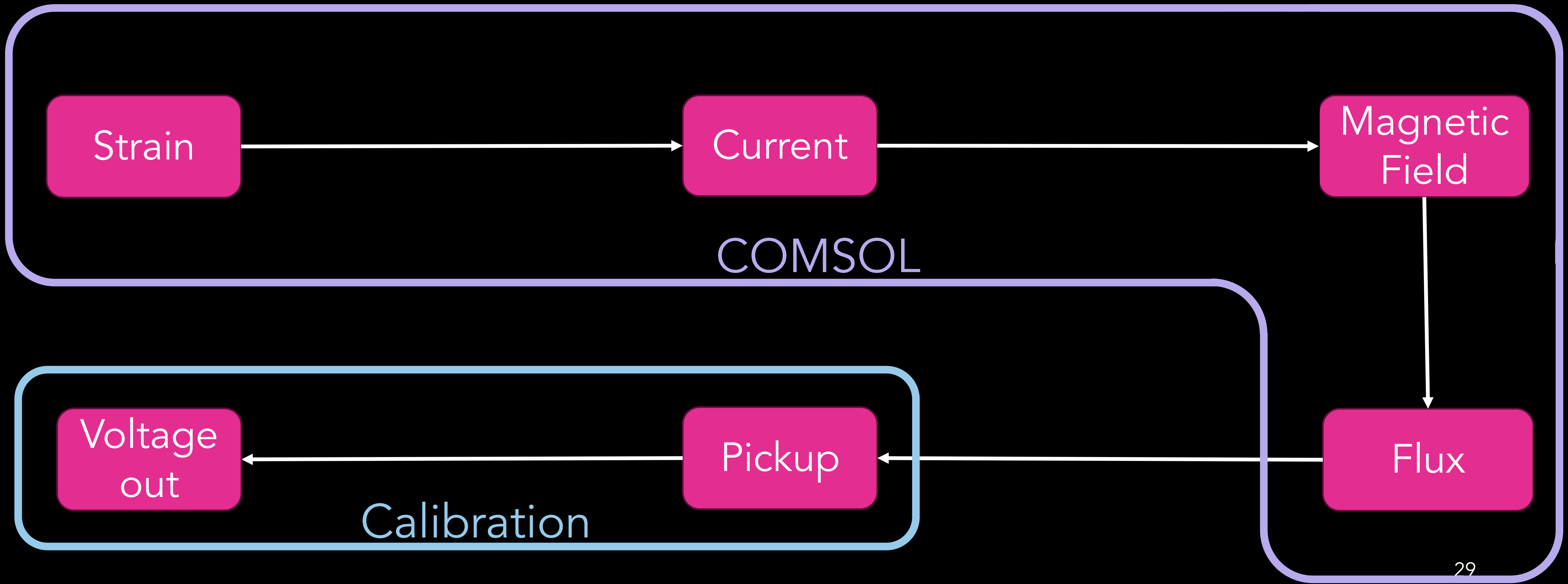

Template Transformation

Need to transform the template into the detector frame

COMSOL:

$$\Phi_{\text{pickup}}(f) = \mathbf{h}^{+/\times}(\omega) \times \omega^2 \times \text{Simulation Results}$$

Calibration:

$$\mathrm{V}_{\text{ADC}}\,(f) = \mathcal{T}(f)_{\Phi_{\text{pickup}} \to \mathrm{V}_{\text{ADC}}} \Phi_{\text{pickup}}(f)$$

COMSOL Flux Simulation

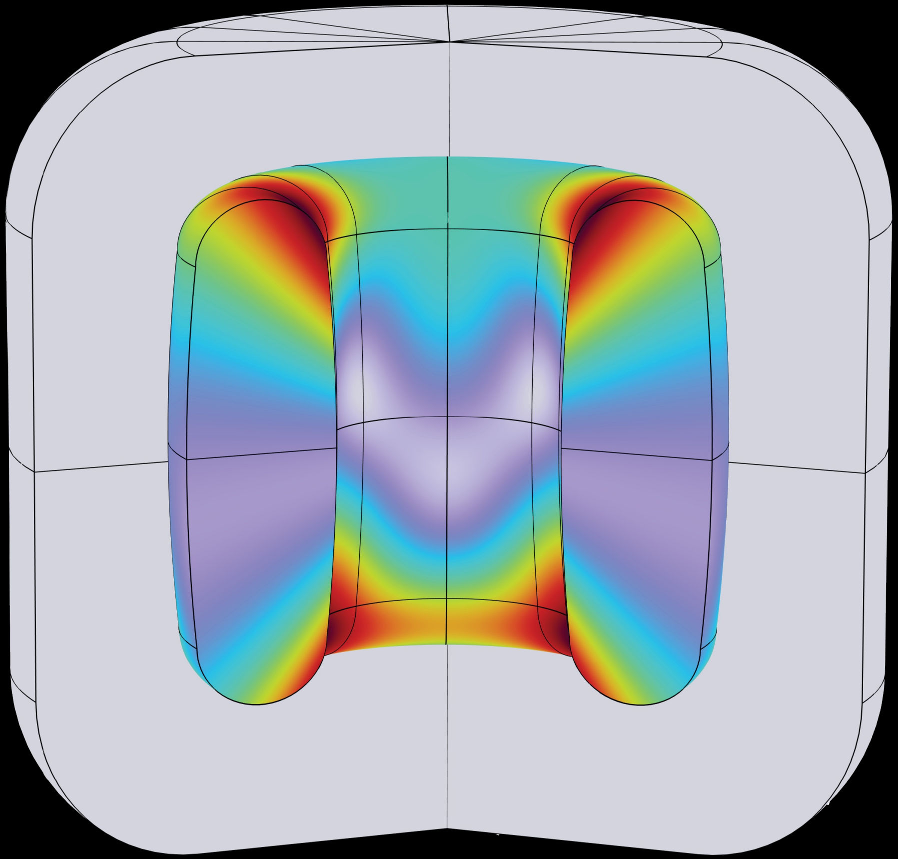

We input the equations for effective current using equations from 2306.03125 for the effective current in a toroidal magnet with extensions to finite height by Sung Mook Lee

COMSOL Flux Simulation

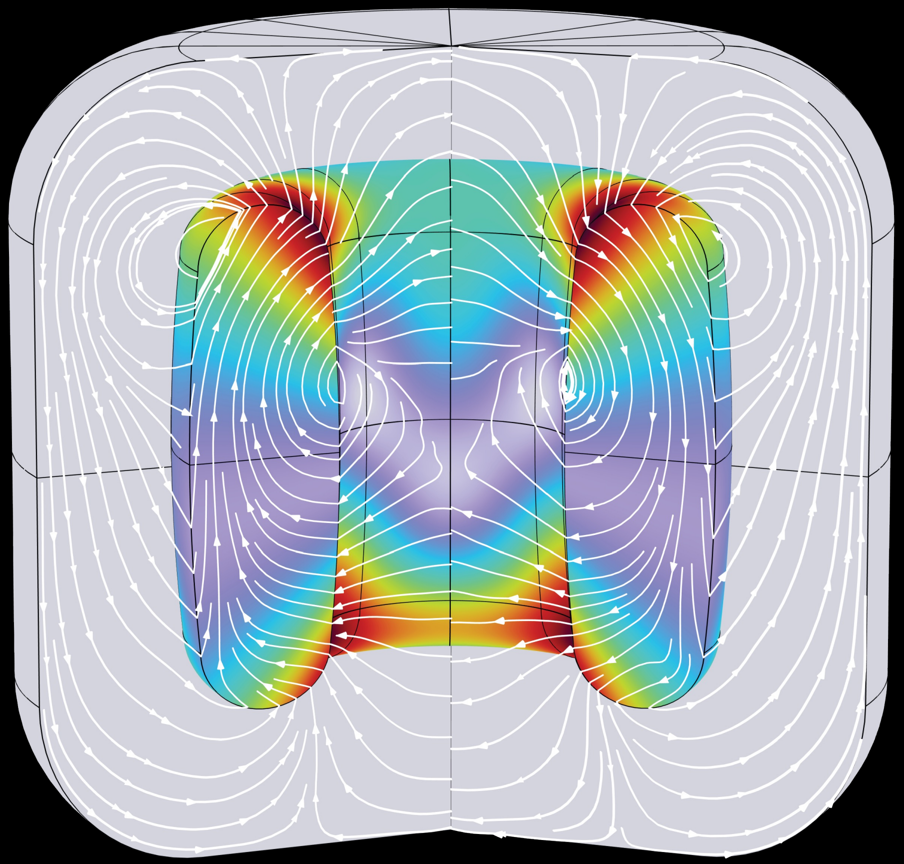

Then we measure the flux generated from the induced magnetic field in the figure-8 area

Strain Polarizations on the Figure-8

The two polarizations of strain are simulated separately over the incoming angle of the signal

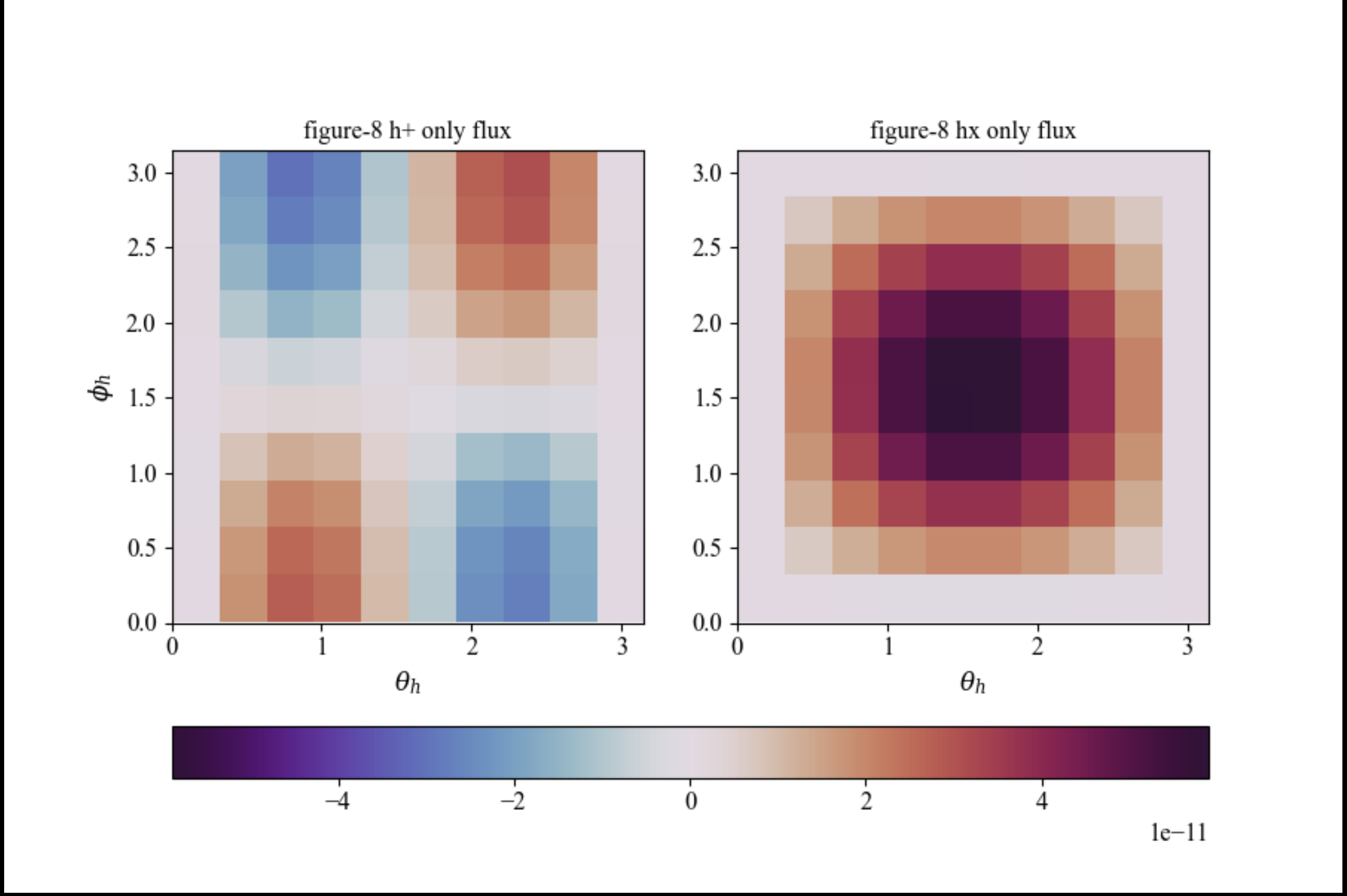

Calibration

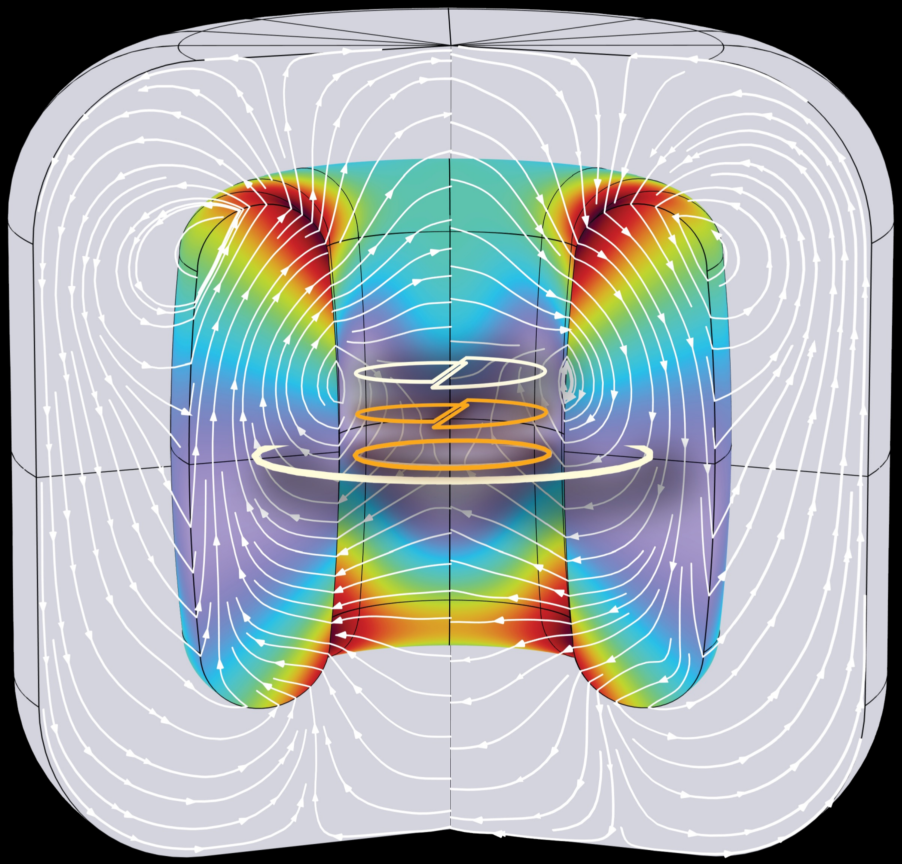

Current in injected into the calibration loops and the response is measured

$$\frac{V_{\mathrm{ADC}}}{V_{\mathrm{sig}}} = \frac{V_{\mathrm{ADC}}}{V_{\mathrm{SQUID}}} \frac{V_{\mathrm{SQUID}}}{V_{\Phi_p}} \frac{V_{\Phi_p}}{I_{\mathrm{C}}} \frac{I_{\mathrm{C}}}{V_{\mathrm{sig}}}$$

Primordial Black Hole Merger Templates

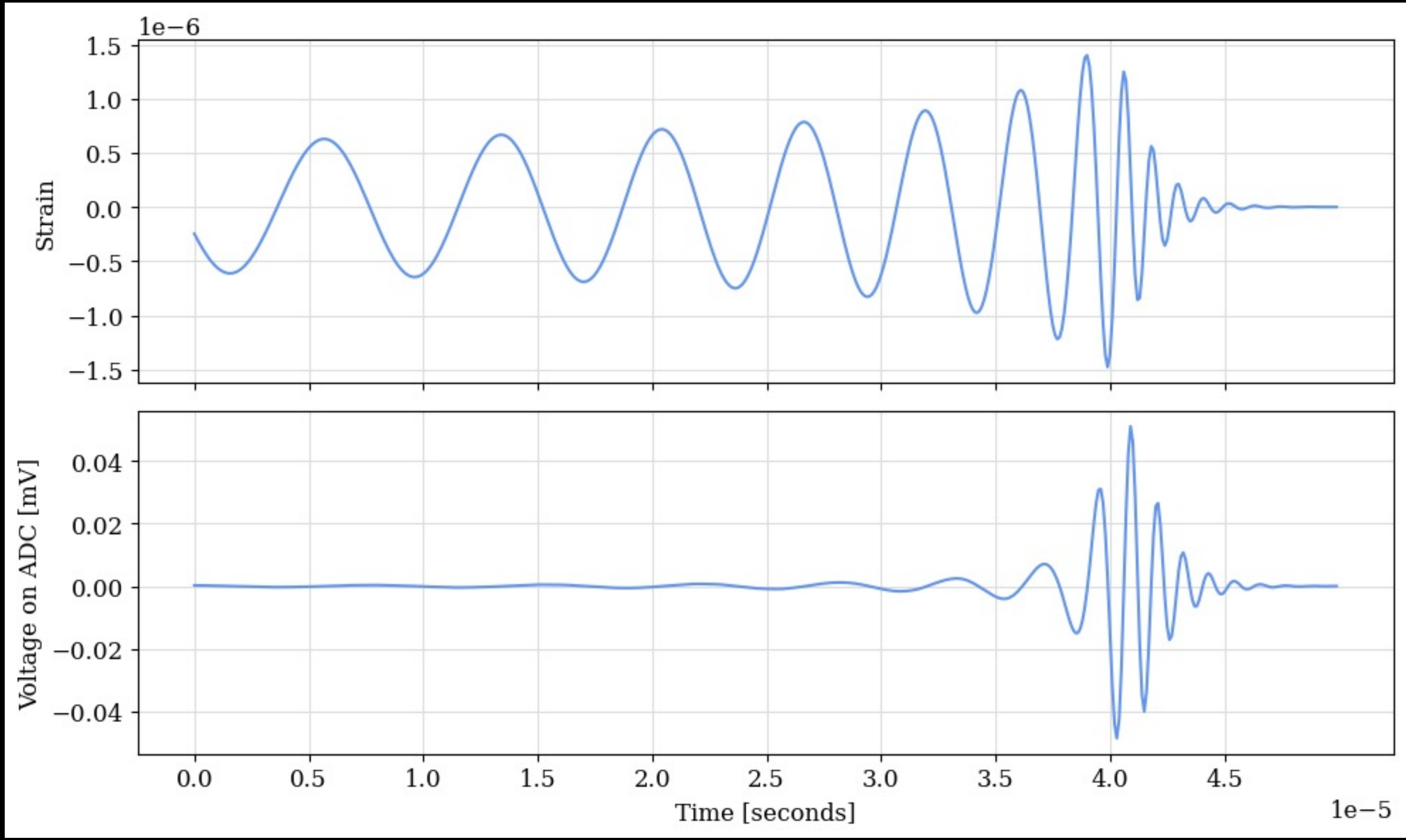

Raw Data

Raw Data

- Data off the digitizer had a bi-modal distribution with spikes.
- Autocorrelation
  - 5 MHz signal is apparent in the data

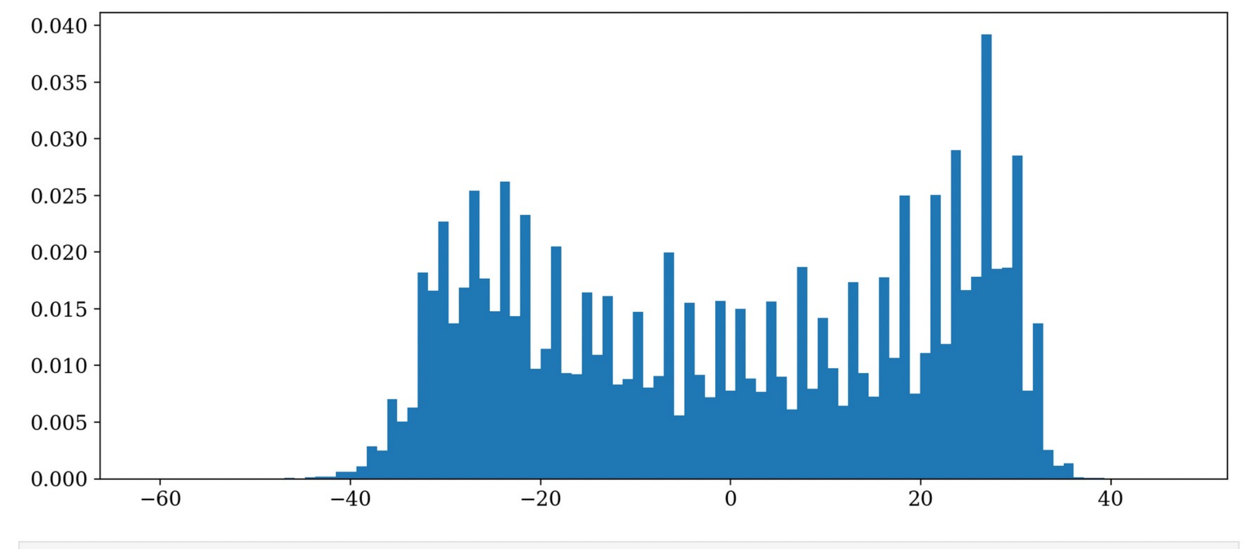

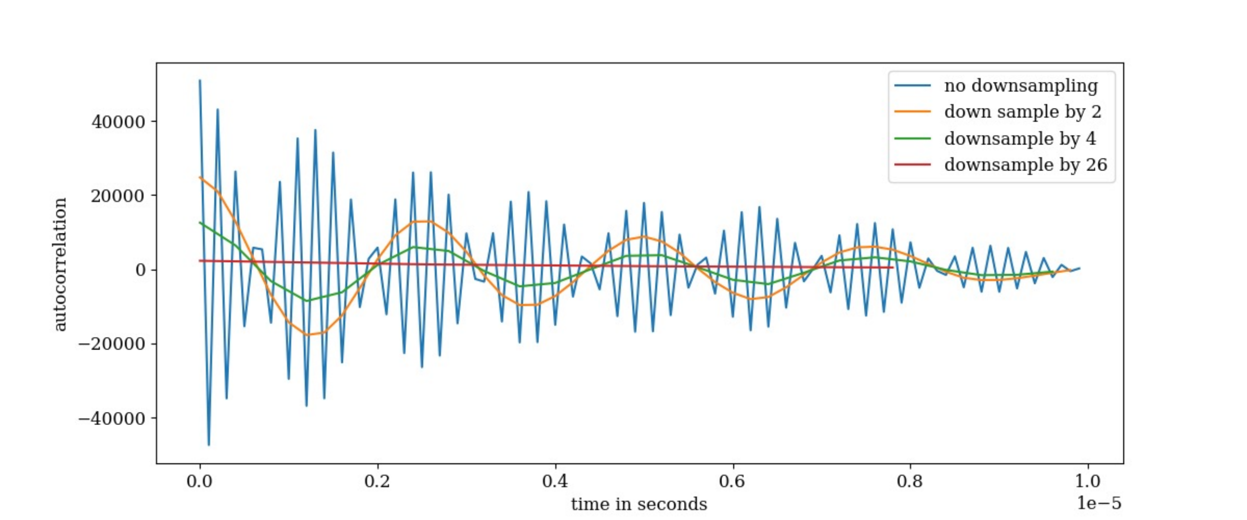

Filtering

After using a Butterworth filter (3 MHz to 10 kHz) distribution *looks* Gaussian

- The Anderson-Darling test failed

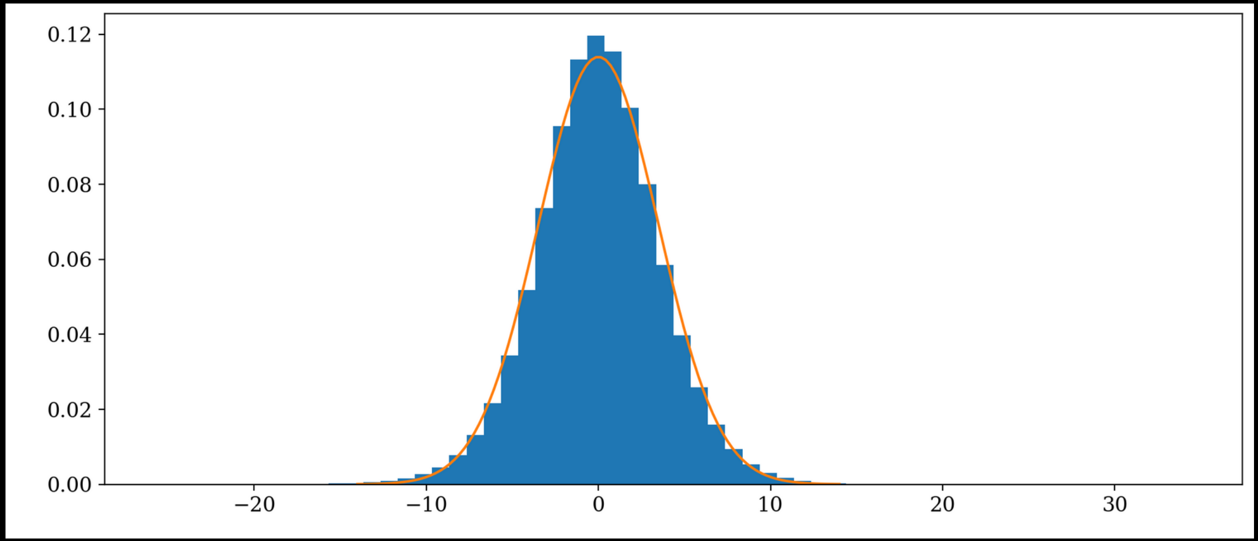

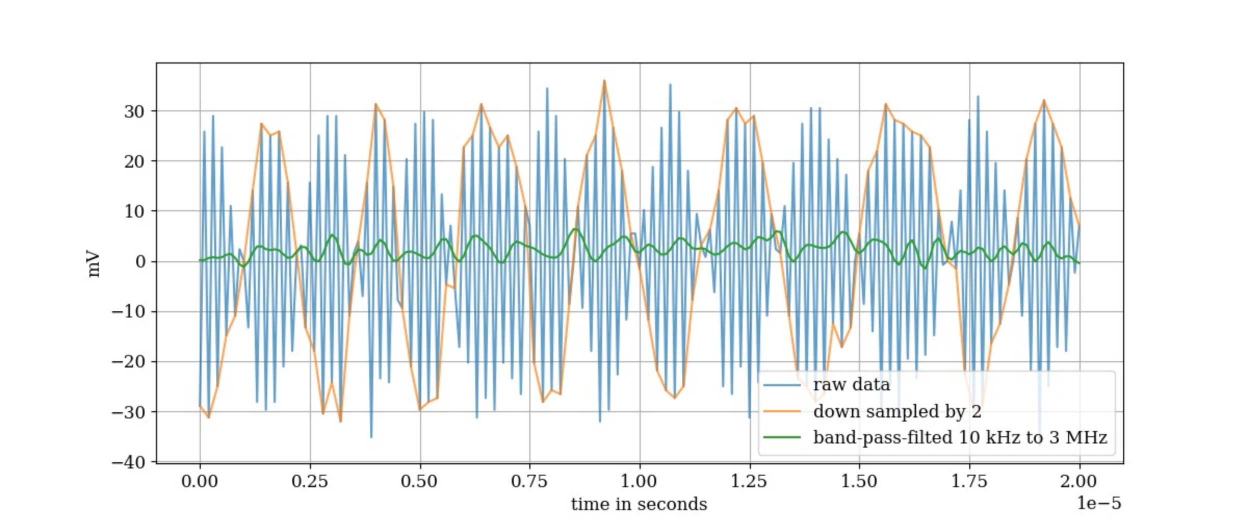

Background Periodic Signal

A 13 kHz background signal remained in the data

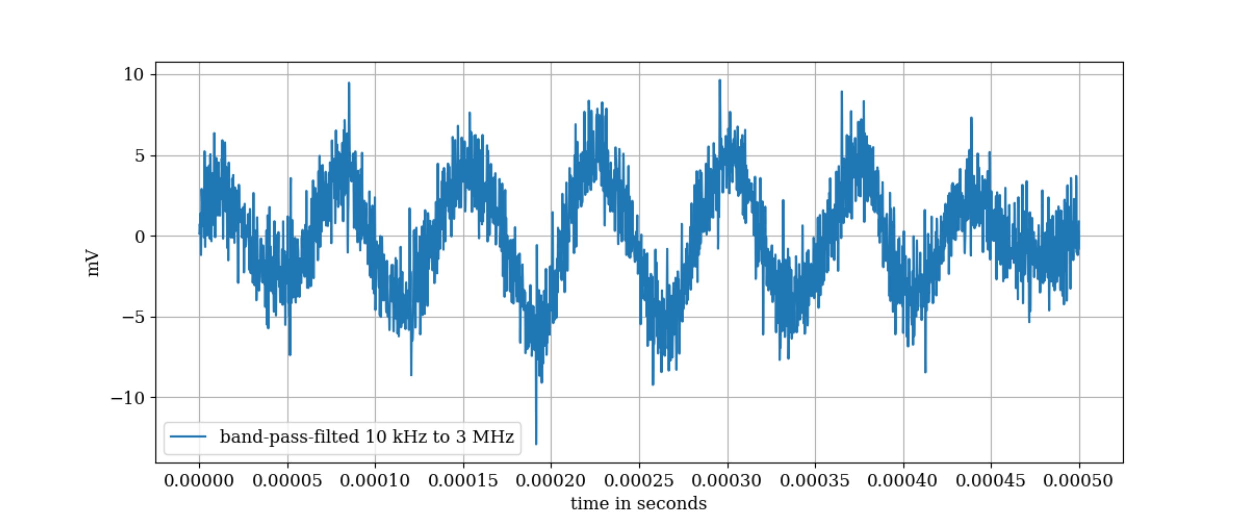

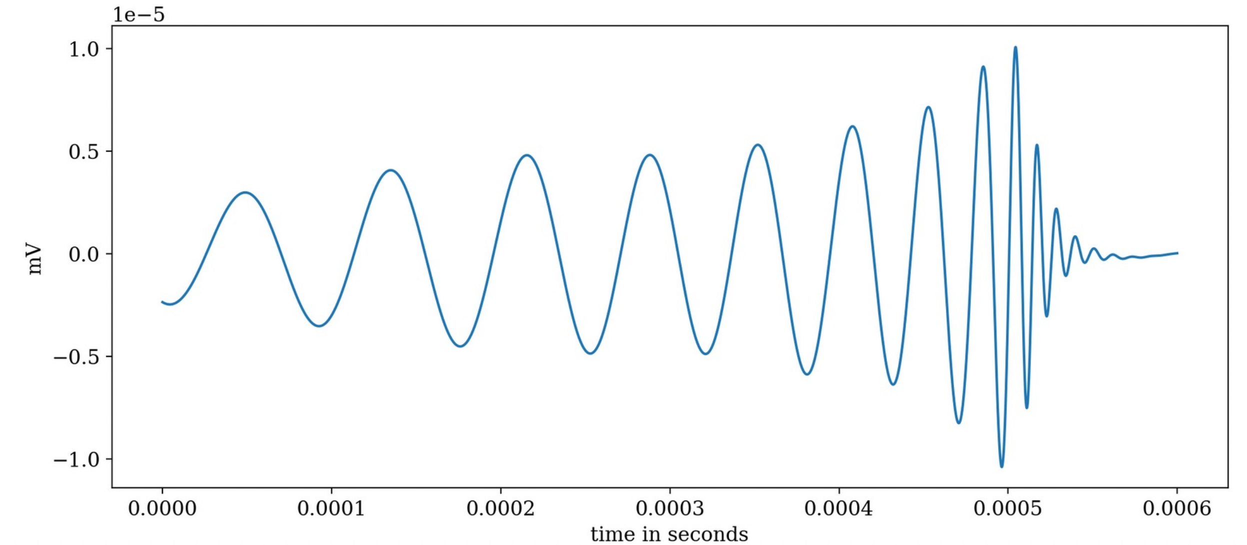

Sensitivity and Stability

Axion Noise Floor

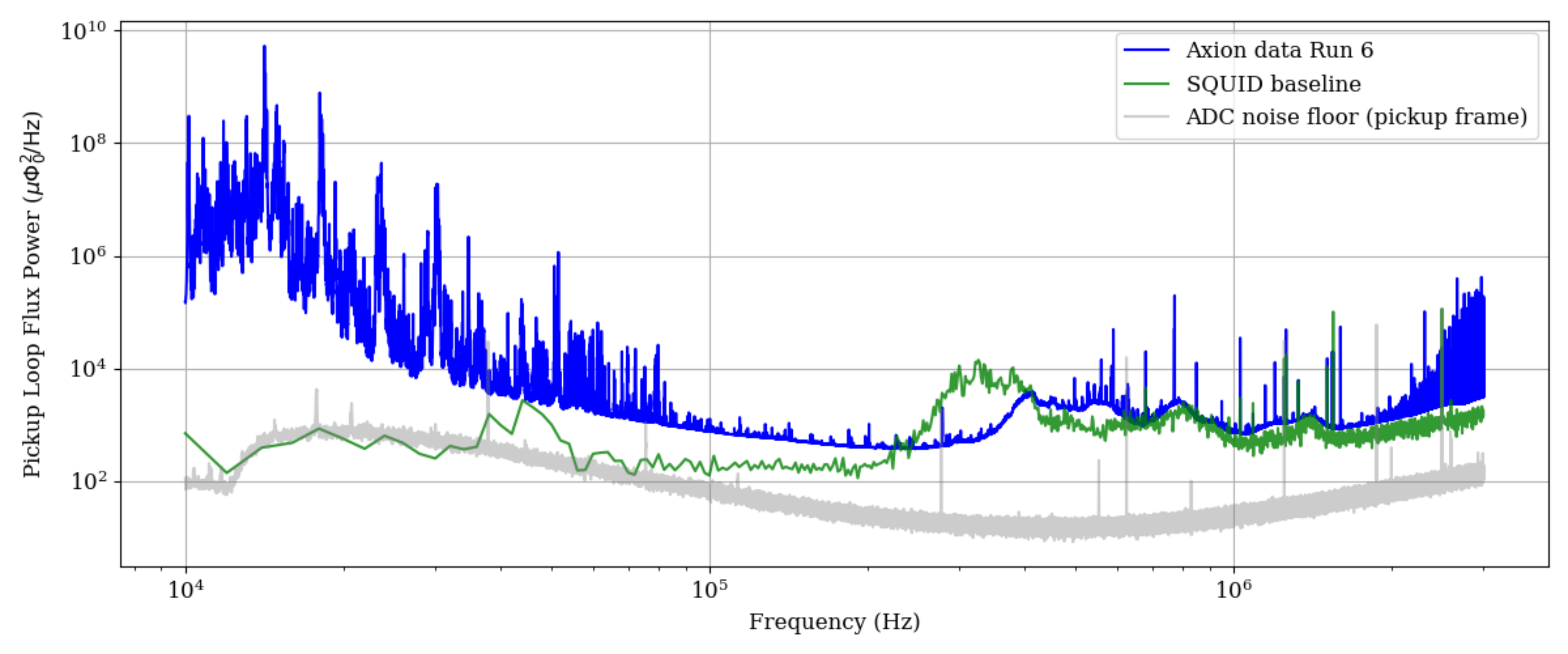

Noise-Equivalent Strain

The noise-equivalent strain sets the detector sensitivity to be able to compare to other detectors in the field

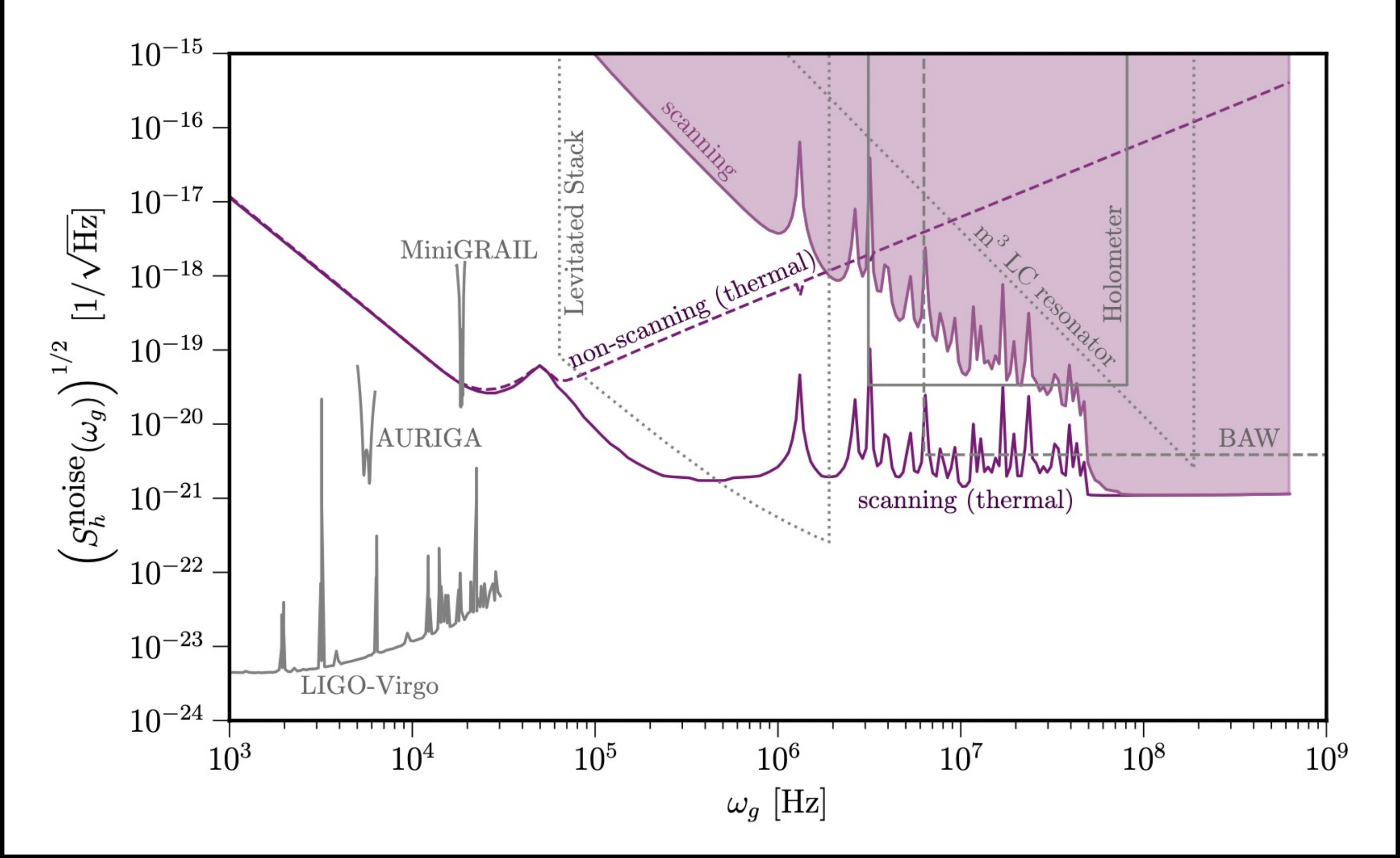

MAGO 2.0 https://arxiv.org/pdf/2303.01518.pdf

Noise-Equivalent Strain

Treat all the noise as if it originated on the detector input $\sqrt{S_n(f)}$

$$S_n(f) = \langle |\tilde{n}(f)|^2 \rangle \Delta f = \sqrt{2}\,\bar{\mathcal{F}}_h(f)$$

$$\mathcal{T}^{-1}(f)^2{}_{\Phi_{\mathrm{pickup}} \to \mathrm{V}_{\mathrm{ADC}}} \bar{\mathcal{F}}_{\mathrm{V}_{\mathrm{ADC}}}(f) = \bar{\mathcal{F}}_{\Phi_{\mathrm{pickup}}}(f)$$

$$\bar{\mathcal{F}}_{\Phi_{\mathrm{pickup}}}(f) \times \left(\mathbf{h}^{+/\times}(\omega) \times \omega^2 \times \text{Simulation Results}\right)^{-2} = \bar{\mathcal{F}}_h(f)$$

Noise-Equivalent Strain

Theoretical calculation performed by Nicholas Rodd

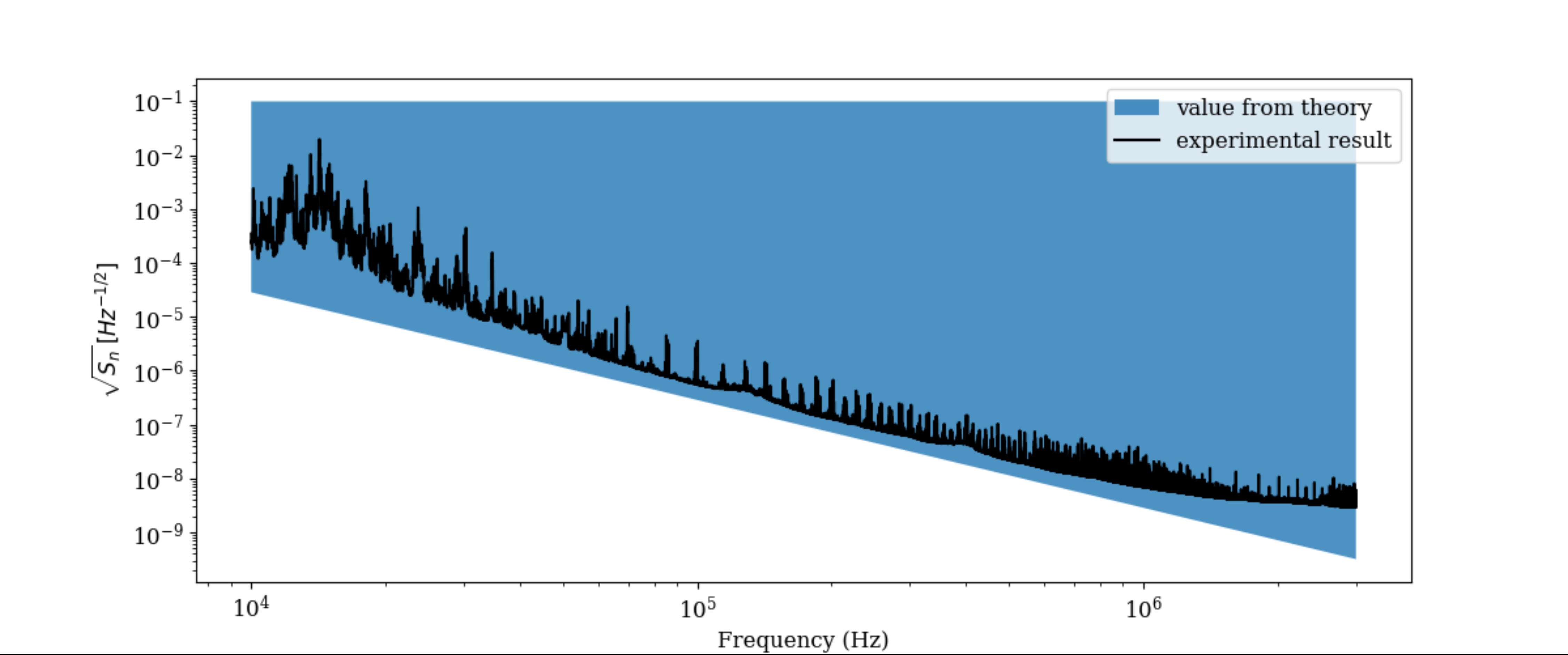

Searching for the Merger Signal

Merger Search

Vary the amplitude of the signal

→ distance and direction of the signal

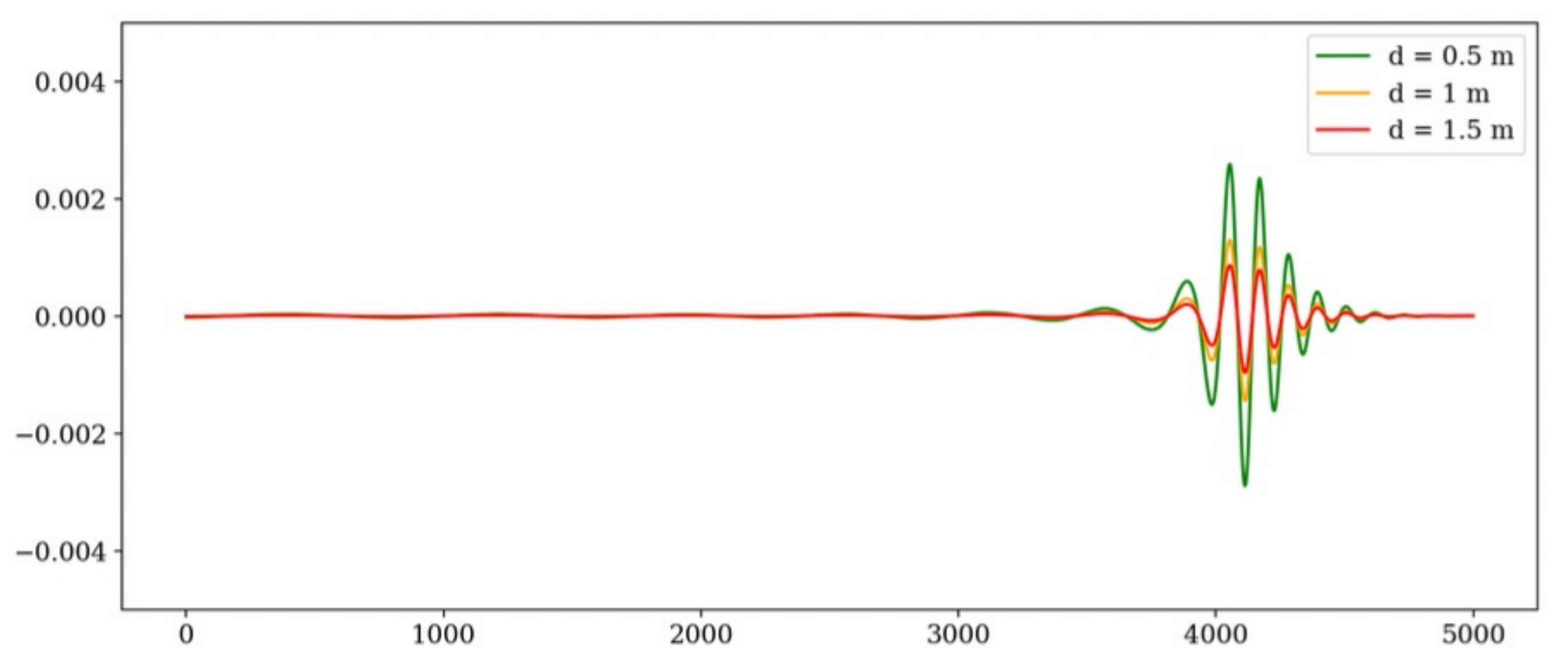

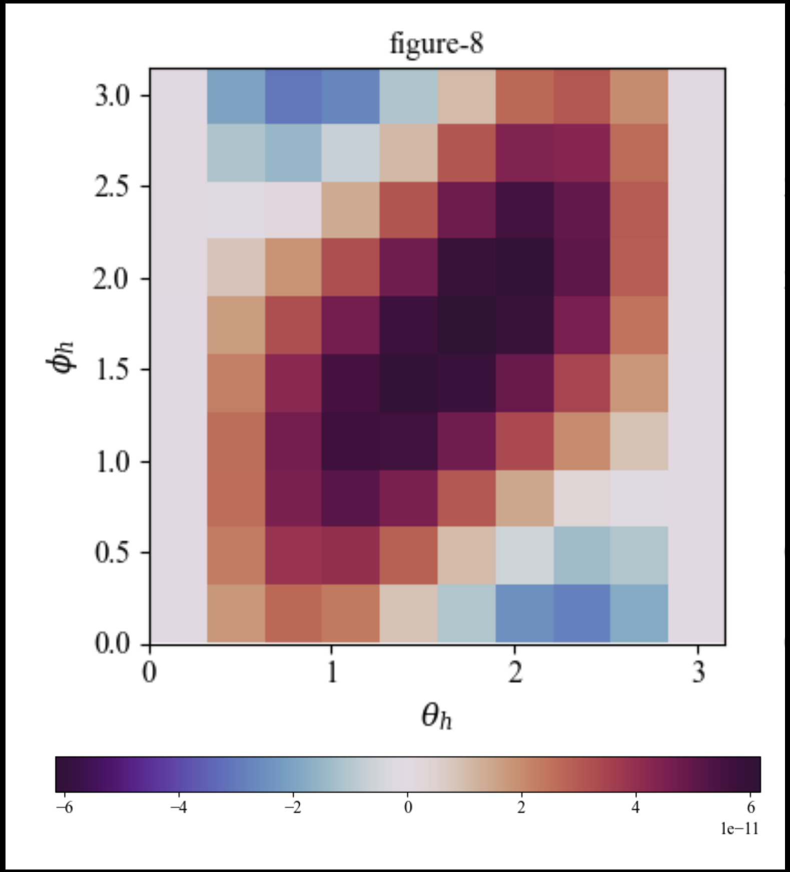

Gaussian Process

Since we have a non-Gaussian background, we cannot use a traditional matched filter

A GP works by fitting multiple distributions to data with a joint Gaussian distribution

$$\begin{bmatrix} f(x) \\ f(x_1) \\ \vdots \\ f(x_n) \end{bmatrix} \sim \mathcal{N}\left(\mu, \begin{bmatrix} k(x,x) & k(x,x_1) & \cdots & k(x,x_n) \\ k(x_1,x) & k(x_1,x_1) & \cdots & k(x_1,x_n) \\ \vdots & \vdots & & \vdots \\ k(x_n,x) & k(x_n,x_1) & \cdots & k(x_n,x_n) \end{bmatrix}\right)$$

Gaussian Process

We choose a covariance matrix (also called a kernel)

$$K\left(\boldsymbol{x}_i, \boldsymbol{x}_j\right) = \mathrm{Cov}\left(f(\boldsymbol{x}_i), f(\boldsymbol{x}_i)\right)$$

For our periodic background we choose a periodic kernel

$$K(\boldsymbol{x}_i, \boldsymbol{x}_j) \; = \exp\left(-\Gamma \sin^2\left[\frac{\pi}{P}\left|\boldsymbol{x}_i - \boldsymbol{x}_j\right|\right]\right)$$

Gaussian Process

The marginalized likelihood for the residuals is given by

$$p(\boldsymbol{r}|t, A) \; = \; N(m(t), K)$$

We can use the marginalized log-likelihood to construct the test statistic

$$\log\big(p(\boldsymbol{r}|t, A)\big) = -\frac{1}{2}\big(\boldsymbol{r}^T \, K^{-1}\boldsymbol{r} + \, \log(\det|K|) + n\log(2\pi)\big)$$

The test statistic is

$$\mathrm{TS} = -2\log\big(p(\boldsymbol{r}|t, A)\big)$$

Signal Injection

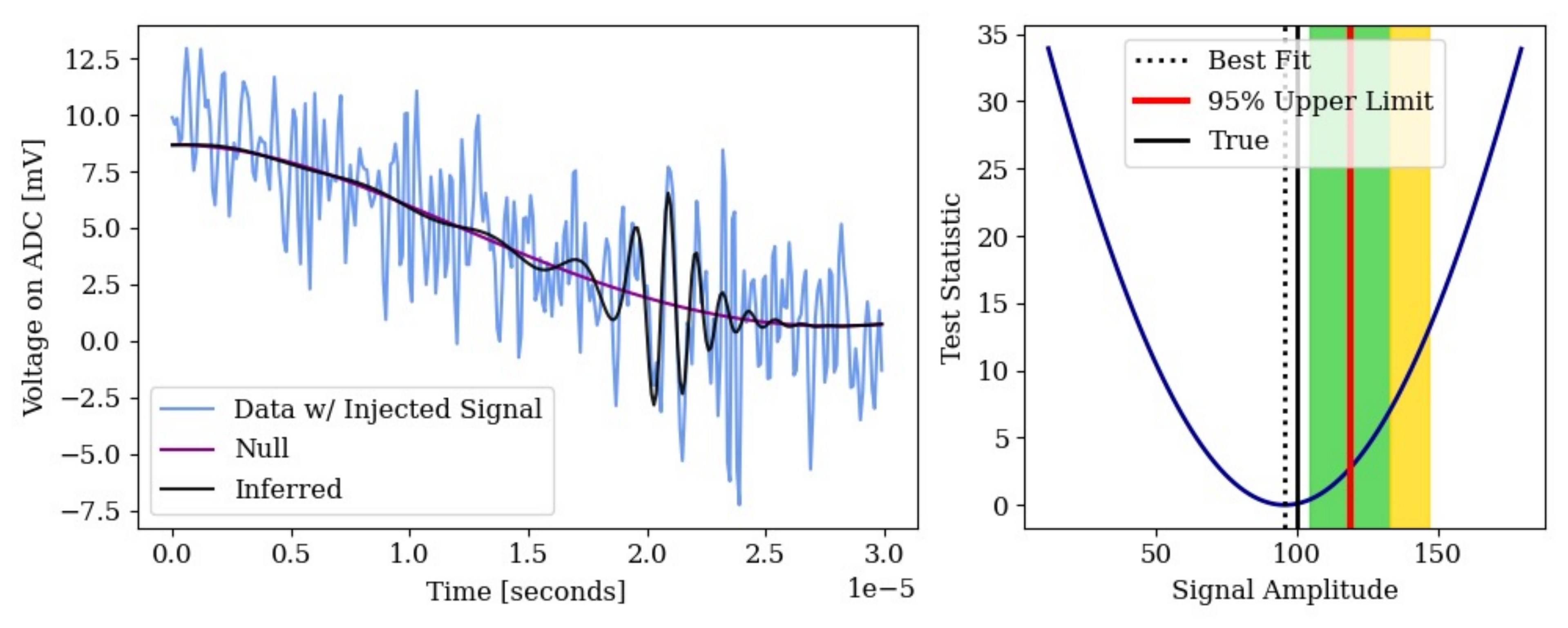

Signal Injection

Varying the injection amplitude over one segment

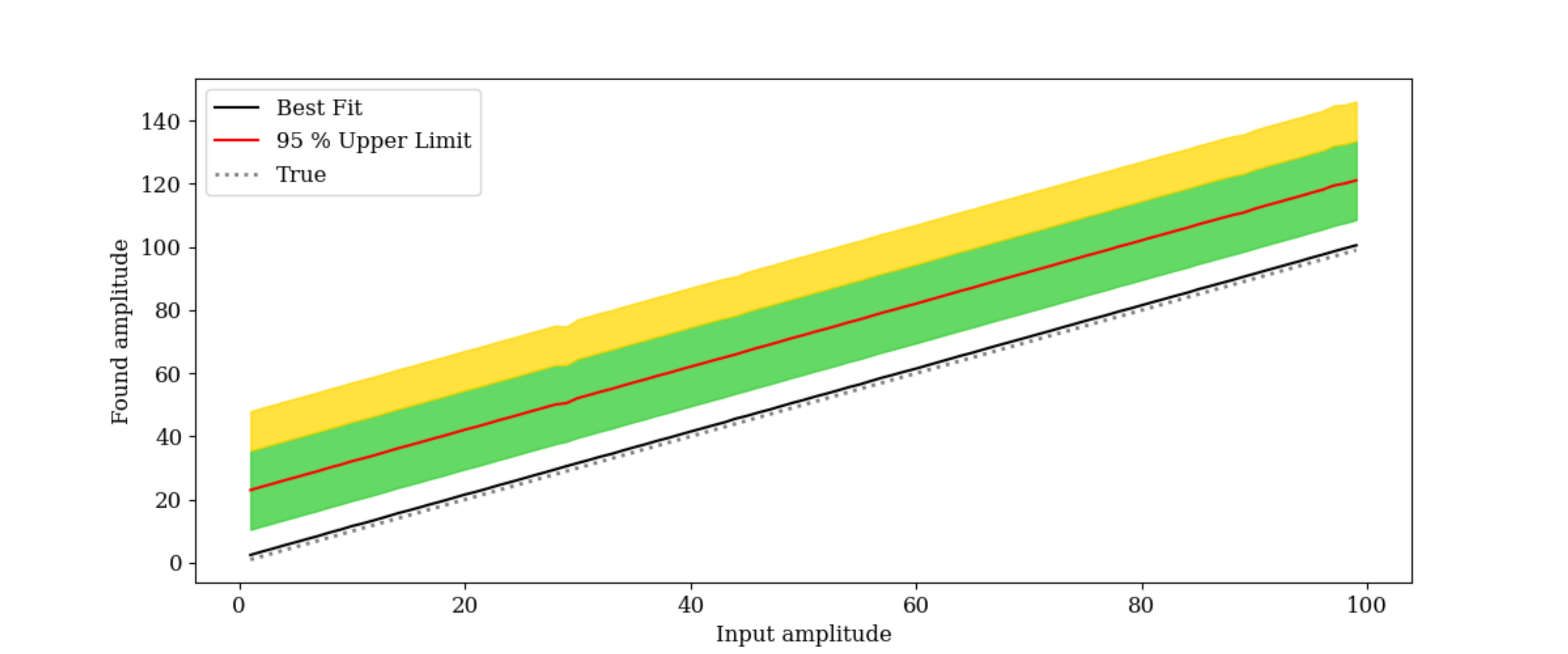

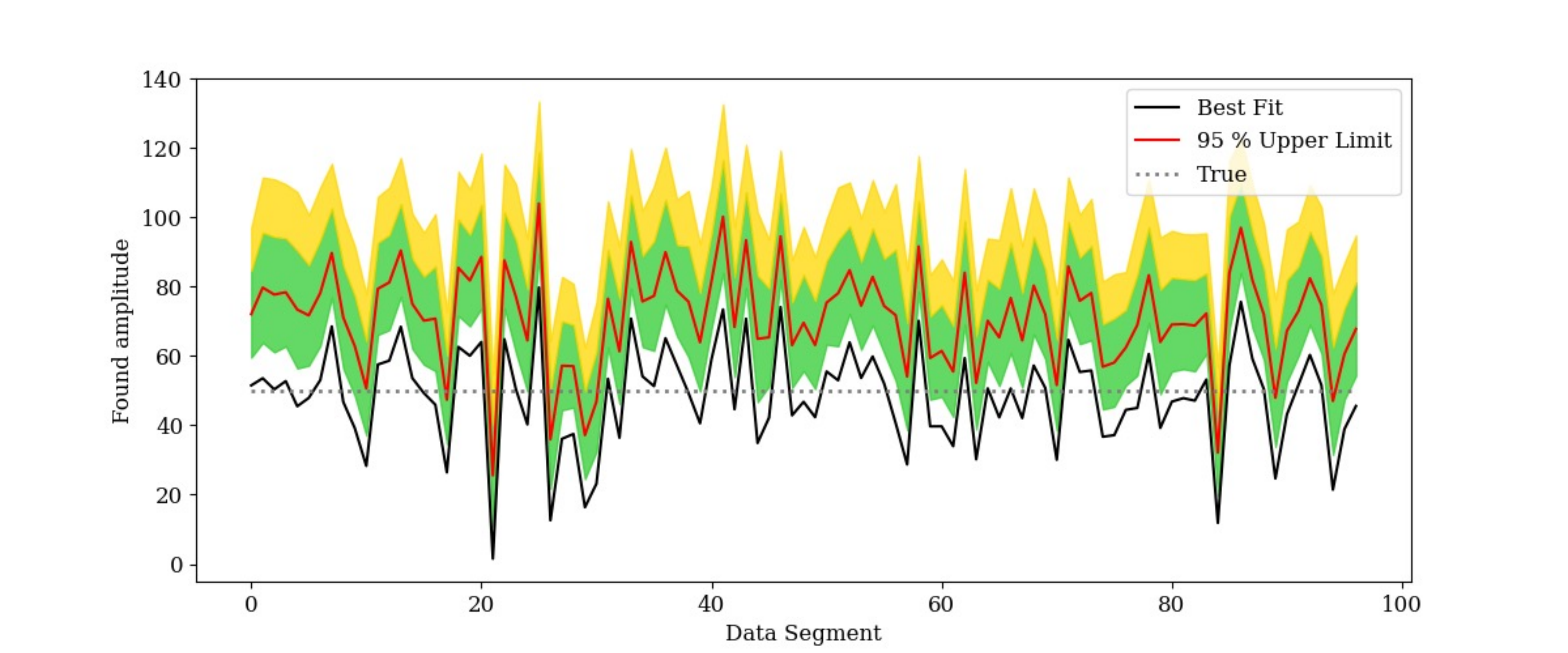

Constant amplitude with varying data segments

Merger Exclusion

Time step $\Delta t = 0.2\,\mu$s

$$N_{\mathrm{process}} = T/\Delta t\ - \left(t_{\mathrm{template}}/\Delta t + 1\right)$$

$$N_{\mathrm{process}} \sim 3 \times 10^{12}$$

Too many steps to process, need alternate approach

Future Searches at High-Frequency

Transient searches: PBH binaries

- Online trigger

Stochastic signals: Astrophysical backgrounds and cosmological signals

- Stationary
- Gaussian distributed
- Isotropic
- Unpolarized

$$h_0^2\Omega_{\rm gw}(f) \simeq 3.6 \left(\frac{n_f}{10^{37}}\right)\left(\frac{f}{1\rm kHz}\right)^4$$

Future Searches: Stochastic signals

For one detector:
$$[\Omega_{\rm GW}(f)]_{\rm min} = \frac{4\pi^2}{3H_0^2} f^3 S_n(f) \frac{(S/N)^2}{F}$$

For two detectors:
$$[\Omega_{\rm GW}(f)]_{\rm min} \sim \frac{4\pi^2}{3H_0^2} \frac{f^3 S_n(f)}{\sqrt{2T\Delta f}} \frac{(S/N)^2}{F}$$

$$\frac{1}{\sqrt{2T\Delta f}} \simeq 1\times 10^{-5} \left(\frac{150\rm Hz}{\Delta f}\right)^{1/2} \left(\frac{1\rm yr}{T}\right)^{1/2}$$

Future Searches: Stochastic signals

ABRA-GW + DMRadio 50 L (in an axion configuration)

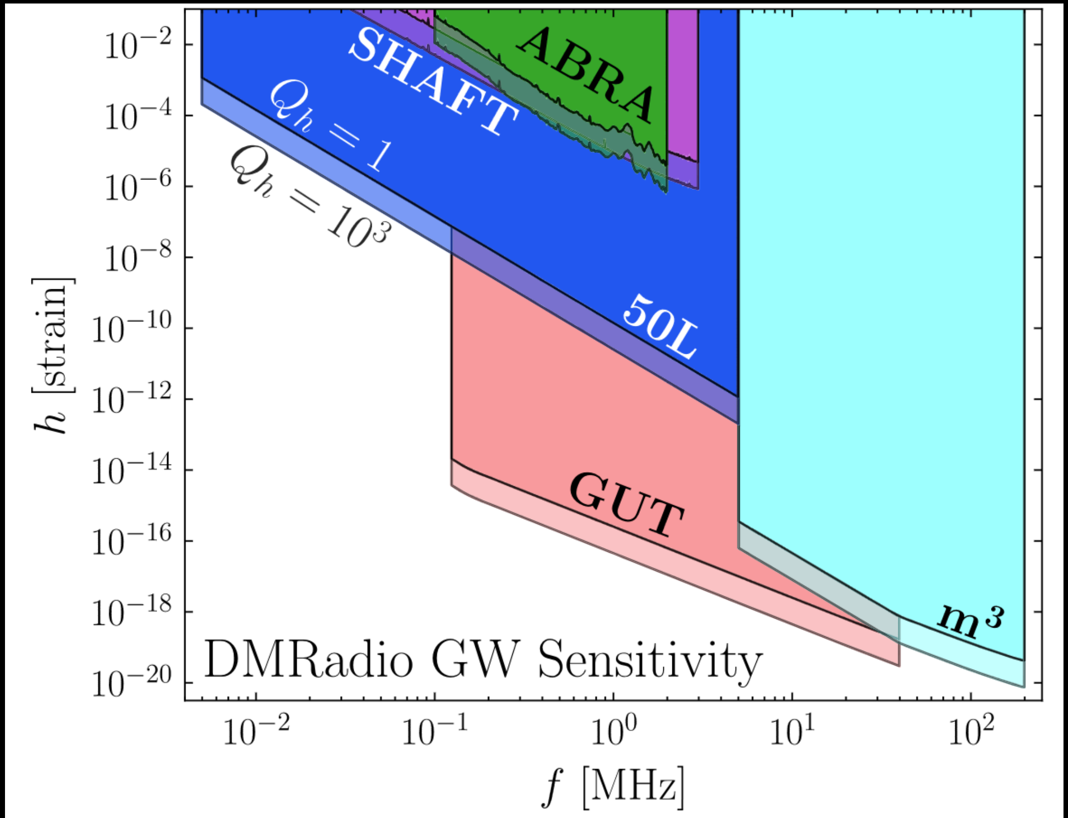

Phys. Rev. Lett. 129, 041101 – Published 20 July 2022: Valerie Domcke, Camilo Garcia-Cely, and Nicholas L. Rodd

Conclusions & Takeaways

- Axions and gravitational waves can both be searched for with electromagnetism
- We modified a lumped-element axion detector to simultaneously detect axions and high-frequency gravitational waves
- Future searches can look for more allusive signals with multiple detectors

Backup Slides

Primordial Black Holes

PBHs were formed before matter domination from over-densities in the plasma

$$\delta > \delta_c = c_s^2$$

Stellar BHs are stellar remnants

→ BHs formed after matter-radiation equality must be larger than 3 $M_\odot$

Primordial Black Holes

Early creation results:

- PBHs could be tiny enough to be DM as a result of Hawking radiation
- PBHs could also be massive, after continuously accreting mass over their lifetime

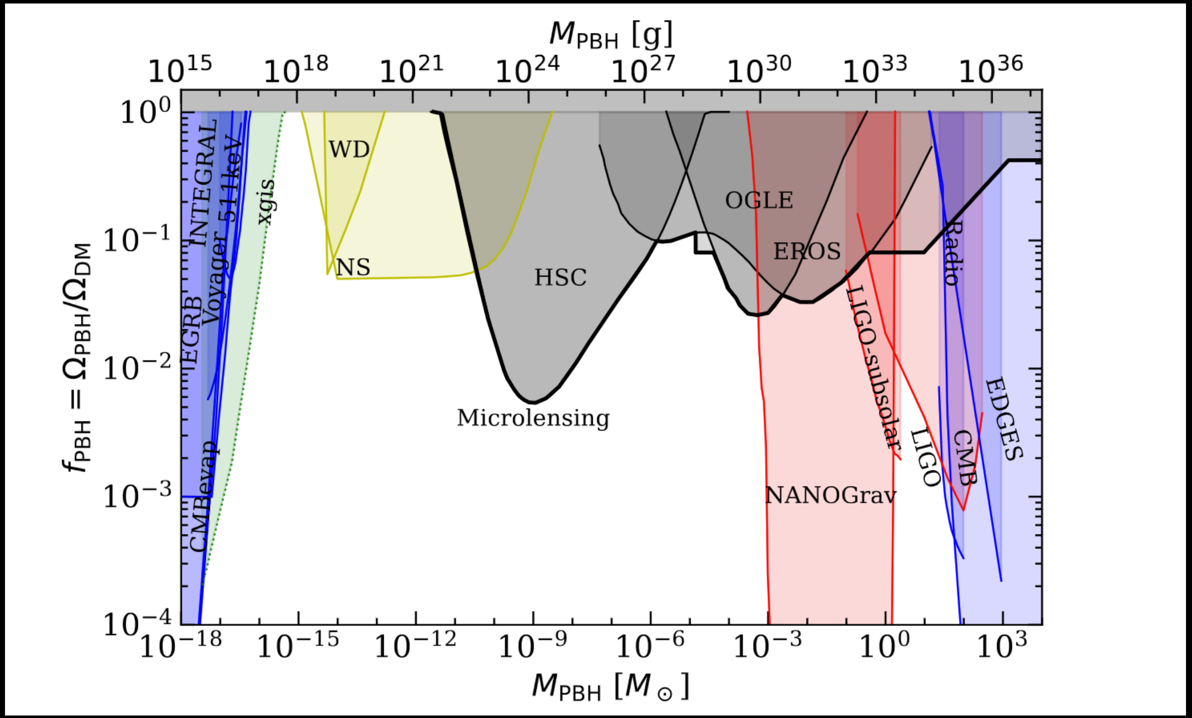

DOI: 10.48550/arXiv.2311.05942
DOI: 10.5281/zenodo.3538999

Primordial Black Hole Binaries

In-spiral

Merger

Ringdown

Primordial Black Hole Binaries

Primordial blackhole in-spiral coherence time:

$$\tau \simeq 0.02\,\mathrm{s}\left(\frac{\mathrm{MHz}}{f}\right)^{8/3}\left(\frac{10^{-5}M_{\odot}}{m}\right)^{5/3}$$

e.g., for f = 10 kHz and τ = 2 days we would be looking for 10^{-6} $M_{\odot}$ PBHs

Axion Signal

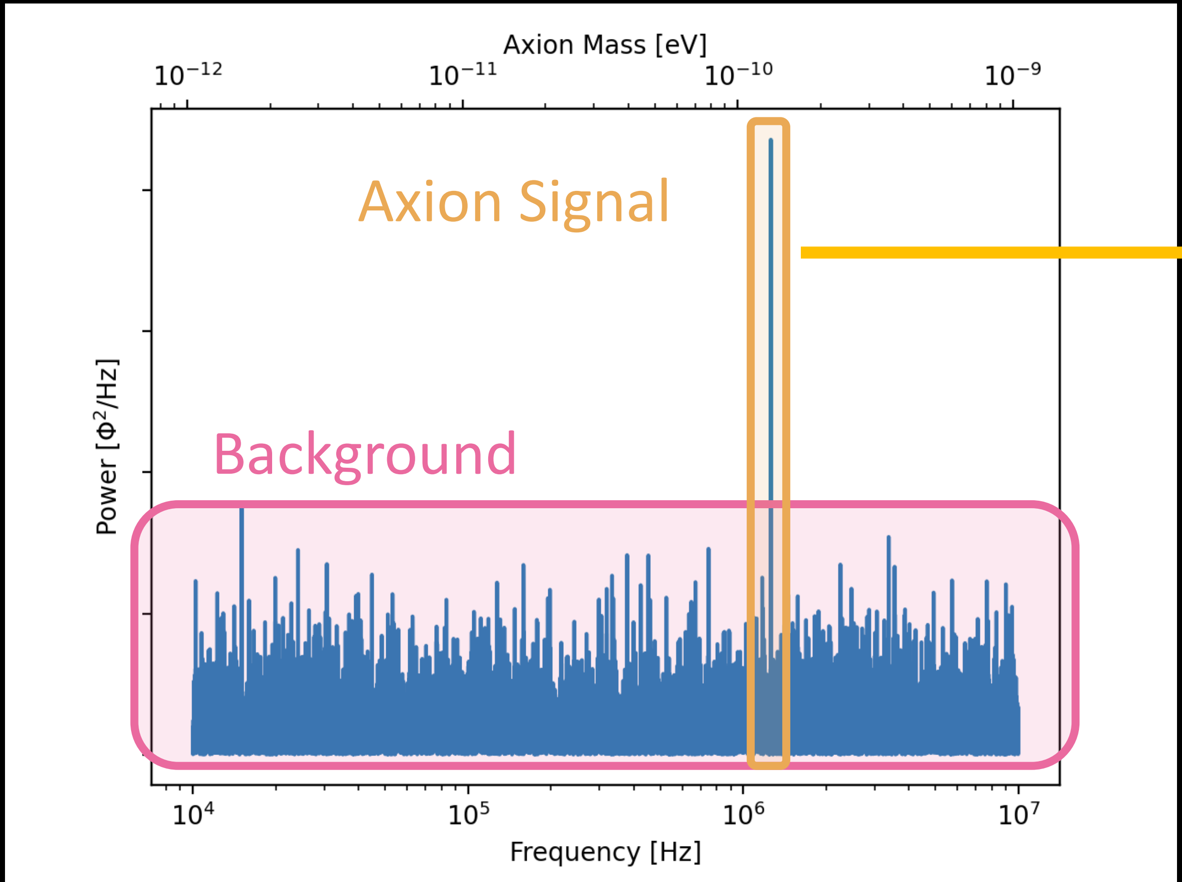

Simulated Data

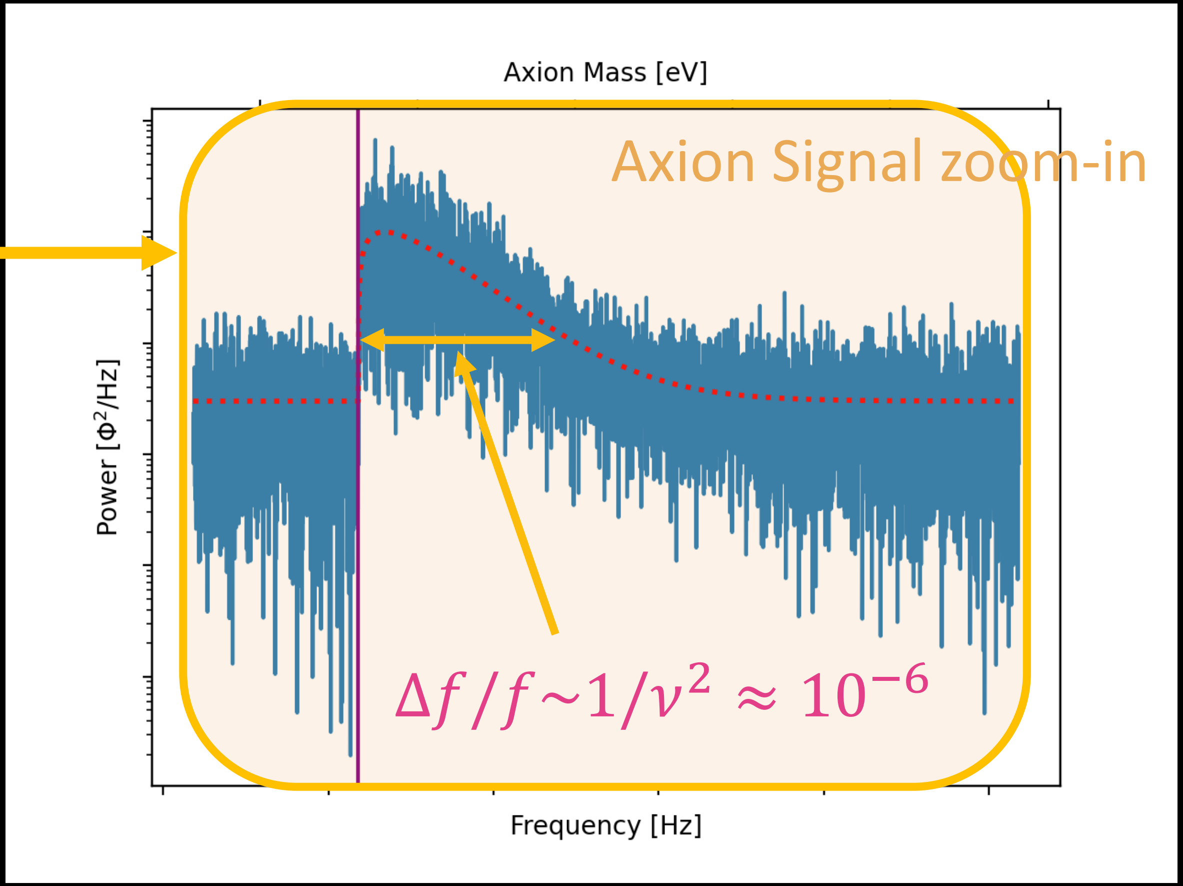

Standard Halo Model

Templates

Testing different mass combinations to see which produces the strongest signal, also cross-correlation tests with white noise

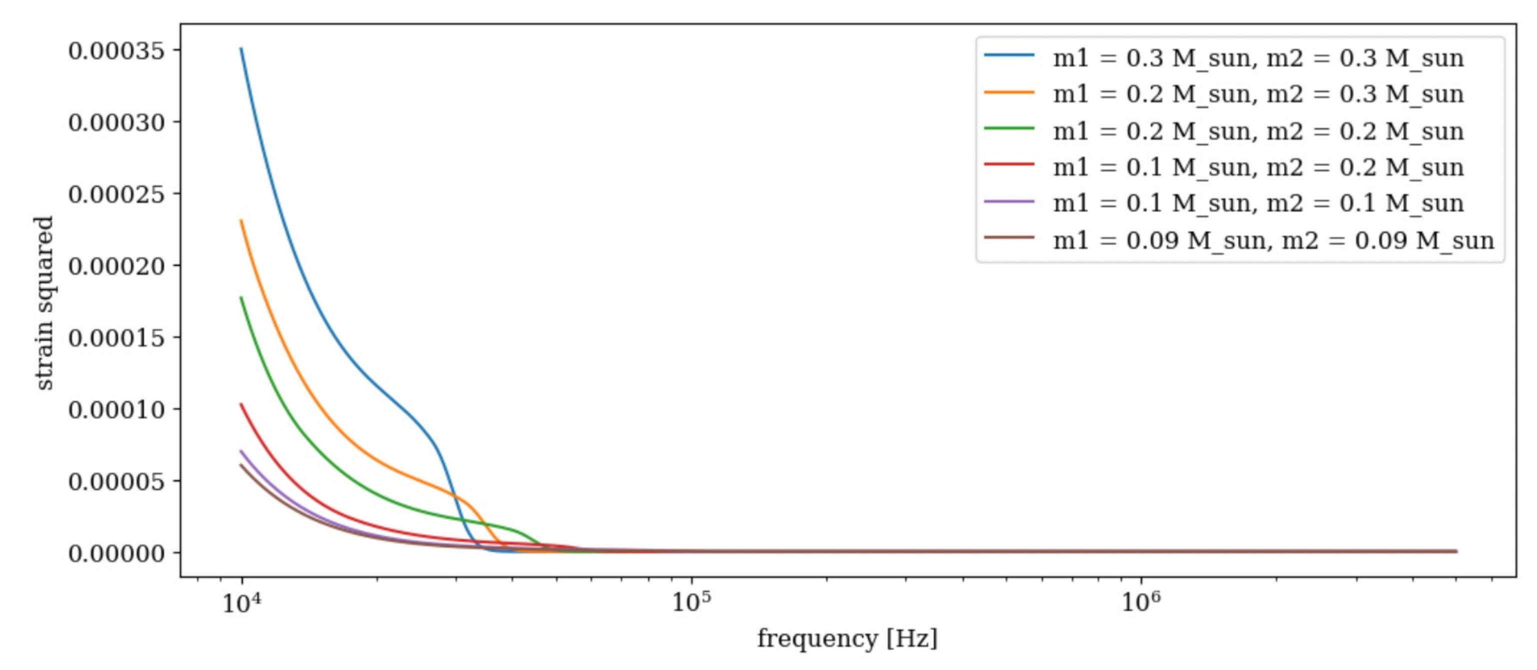

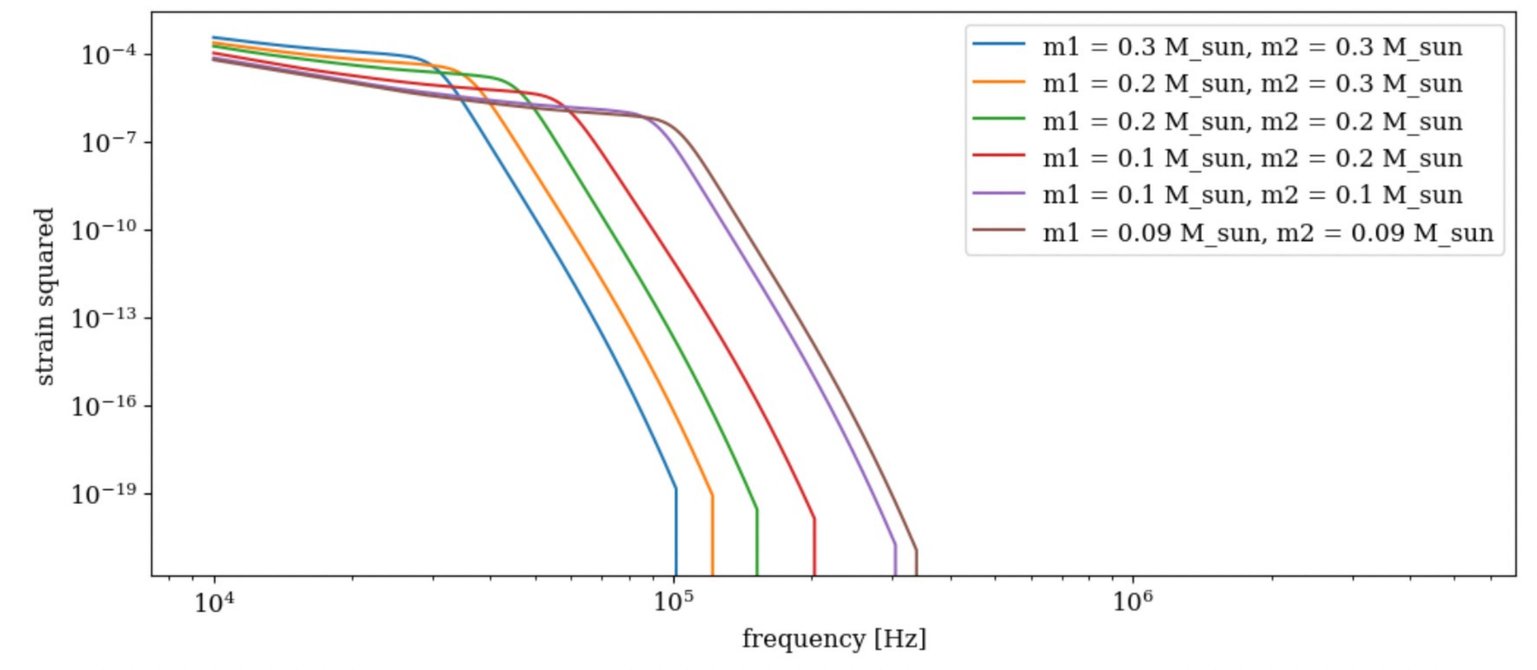

Signal to noise ratio

$$SNR = g_{a\gamma\gamma}\sqrt{\rho_{DM}}\mathcal{G}VB_{max}\left(\frac{M_{in}}{L_T}\right)\frac{(\tau t)^{1/4}}{{S_{\Phi\Phi}}^{1/2}}$$

Signal to noise ratio

$$SNR = g_{a\gamma\gamma}\sqrt{\rho_{DM}}\, g V B_{max} \left(\frac{M_{in}}{L_T}\right) \frac{(\tau t)^{1/4}}{{S_{\Phi\Phi}}^{1/2}}$$

Axion to photon coupling constant

Local dark matter density

Signal to noise ratio

$$SNR = g_{a\gamma\gamma}\sqrt{\rho_{DM}}\boxed{\mathcal{G}}VB_{max}\left(\frac{M_{in}}{L_T}\right)\frac{(\tau t)^{1/4}}{S_{\Phi\Phi}{}^{1/2}}$$

Geometric factor

Signal to noise ratio

$$SNR = g_{a\gamma\gamma}\sqrt{\rho_{DM}}\,\boxed{\mathcal{G}V}\,\boxed{B_{max}}\left(\frac{M_{in}}{L_T}\right)\frac{(\tau t)^{1/4}}{S_{\Phi\Phi}{}^{1/2}}$$

Magnetic field volume

Maximum value of the magnetic field

Signal to noise ratio

$$SNR = g_{a\gamma\gamma}\sqrt{\rho_{DM}}\mathcal{G}VB_{max}\boxed{\left(\frac{M_{in}}{L_T}\right)}\frac{(\tau t)^{1/4}}{S_{\Phi\Phi}{}^{1/2}}$$

Inductive coupling of the SQUIDs

Signal to noise ratio

$$SNR = g_{a\gamma\gamma}\sqrt{\rho_{DM}}\mathcal{G}V B_{max}\left(\frac{M_{in}}{\boxed{L_T}}\right)\frac{(\tau t)^{1/4}}{{S_{\Phi\Phi}}^{1/2}}$$

Inductive coupling to the readout circuit

Signal to noise ratio

$$SNR = g_{a\gamma\gamma}\sqrt{\rho_{DM}}\mathcal{G}VB_{max}\left(\frac{M_{in}}{L_T}\right)\frac{(\tau t)^{1/4}}{S_{\Phi\Phi}^{1/2}}$$

Axion coherence time and the integration time

Signal to noise ratio

$$SNR = g_{a\gamma\gamma}\sqrt{\rho_{DM}}\mathcal{G}V B_{max}\left(\frac{M_{in}}{L_T}\right)\frac{(\tau t)^{1/4}}{\boxed{S_{\Phi\Phi}}^{1/2}}$$

Flux noise level/ noise on our SQUIDs

Signal to noise ratio

$$SNR = g_{a\gamma\gamma}\sqrt{\rho_{DM}}\mathcal{G}VB_{max}\boxed{\left(\frac{M_{in}}{L_T}\right)}\frac{(\tau t)^{1/4}}{S_{\Phi\Phi}{}^{1/2}}$$

Coupling of SQUIDS to axion signal through the pickup structure